REPORT DOCUMENTATION PAGE

Form Approved OMB NO. 0704-0188

1. REPORT DATE (DD-MM-YYYY)	2. REPORT TYPE	3. DATES COVERED (From - To)
05-09-2022	Final Report	7-May-2019 - 6-Sep-2022

4. TITLE AND SUBTITLE
Final Report: Probing direct cell-to-cell exchange of matter in a Clostridium syntrophic coculture

5a. CONTRACT NUMBER
W911NF-19-1-0274

5b. GRANT NUMBER

5c. PROGRAM ELEMENT NUMBER
611102

6. AUTHORS

5d. PROJECT NUMBER

5e. TASK NUMBER

5f. WORK UNIT NUMBER

7. PERFORMING ORGANIZATION NAMES AND ADDRESSES
University of Delaware
210 Hullihen Hall

Newark, DE 19716 -0099

8. PERFORMING ORGANIZATION REPORT NUMBER

9. SPONSORING/MONITORING AGENCY NAME(S) AND ADDRESS (ES)
U.S. Army Research Office
P.O. Box 12211
Research Triangle Park, NC 27709-2211

10. SPONSOR/MONITOR'S ACRONYM(S)
ARO

11. SPONSOR/MONITOR'S REPORT NUMBER(S)
74827-BB.1

12. DISTRIBUTION AVAILIBILITY STATEMENT
Approved for public release; distribution is unlimited.

13. SUPPLEMENTARY NOTES
The views, opinions and/or findings contained in this report are those of the author(s) and should not contrued as an official Department of the Army position, policy or decision, unless so designated by other documentation.

14. ABSTRACT

15. SUBJECT TERMS

16. SECURITY CLASSIFICATION OF:			17. LIMITATION OF ABSTRACT	15. NUMBER OF PAGES	19a. NAME OF RESPONSIBLE PERSON
a. REPORT	b. ABSTRACT	c. THIS PAGE			Eleftherios Papoutsakis
UU	UU	UU	UU		19b. TELEPHONE NUMBER 302-831-8376

RPPR Final Report
as of 08-Dec-2022

Agency Code: 21XD

Proposal Number: 74827BB **Agreement Number: W911NF-19-1-0274**
INVESTIGATOR(S):

Name: Eleftherios Papoutsakis
Email: epaps@udel.edu
Phone Number: 3028318376
Principal: Y

Organization: **University of Delaware**
Address: 210 Hullihen Hall, Newark, DE 197160099
Country: USA

DUNS Number: 059007500 EIN: 516000297
Report Date: 06-Dec-2022 Date Received: 05-Sep-2022
Final Report for Period Beginning 07-May-2019 and Ending 06-Sep-2022
Title: Probing direct cell-to-cell exchange of matter in a Clostridium syntrophic coculture
Begin Performance Period: 07-May-2019 **End Performance Period:** 06-Sep-2022
Report Term: 0-Other

Submitted By: Eleftherios Papoutsakis Email: epaps@udel.edu
Phone: (302) 831-8376

Distribution Statement: 1-Approved for public release; distribution is unlimited.

STEM Degrees: 3 **STEM Participants:** 4

Major Goals: The goal of this ARO project is to dissect at the cellular a binary Clostridium syntrophic co-culture that exhibits unusual and previously unreported phenomena of cell fusion and direct exchange of matter between the two microbes, based on data developed under the support of an ARO STIR grant. The syntrophic system is made up of Clostridium acetobutylicum (Cac), which converts simple and complex carbohydrates into solvents and carboxylates, and the acetogen C. ljungdahlii (Clj) which fixes CO2. Direct cell-to-cell interactions and material exchange among the two microbes enabled unforeseen metabolic rearrangements. Evidence for direct cell-to-cell interactions was provided using metabolic analysis, fluorescence microscopy (FM) and electron microscopies (TEM & SEM). This includes strong evidence for cell-wall and membrane fusion events and exchange of small molecules, reducing equivalents (electrons) and macromolecules. Here we will test hypotheses aiming to dissect these novel interactions using correlative FM/TEM/SEM and immunogold and/or related nanogold-based electron microscopies to detail the exchange of macromolecules. We will also probe possible direct transfer of nucleic acids (RNA and plasmid DNA) from Cac to Clj. We will use genetic and culture modifications to identify the mechanism by which Cac transfers reducing equivalent (“electrons”) to Clj: if through direct transport of H2 or by direct transport of electron-carrier proteins or by generating an artificial interspecies electron-transport chain. Cellular-level understanding of this syntrophy, as proposed here, could lead to many fundamental and practical findings, with applications in environmental sustainability, remediation, the study of natural and synthetic ecosystems and microbiomes, and how they can be used to produce chemicals and fuels from renewable biomass and waste materials, including CO2, H2 and syngas that can be generated from various sources. Such applications are of interest to ARO as impacting defense-related operations. This grant will support graduate students working in the PI’s lab.

Accomplishments: We accomplished goals from both Aim 1 and 2. For details see attached report.
For Aim 1, we developed two new anerobic fluorescent reporters, HaloTag and SNAP-tag for anaerobic labeling in both C. acetobutuylicm and C. ljungdahlii. We also showed that HaloTag (with Janelia 646 fluorogen) and SNAP-tag (with 647-SiR fluorogen) show orthogonal fluorescence labeling when co-incubated with FAST and HMBR using flow cytometry. To determine if C. ljungdahlii can express anaerobic fluorescent fusion proteins we also expressed Cac ZapA-FAST in Clj, showing evidence of the first fluorescent fusion protein expressed in Clj. We also showed that there is exchange of the whole proteome between C. acetobutylicum and C. ljungdahlii in co-culture using CellTracker DeepRed dye to label C. ljungdahlii proteins and C. acetobutylicum expressing ZapA-FAST labeled with the HMBR fluorogen. We also showed the two organisms massively exchange cellular RNA in co-culture. We showed evidence of a novel type of horizontal gene transfer between C. acetobutylicum and C. ljundaglii in co-culture. Evidence of integration of a portion of the p100ptaHalo plasmid was transferred from C. ljungdahlii to strain C. acetobutylicum.

RPPR Final Report
as of 08-Dec-2022

For Aim 2 We created a Cac Fd-FAST fluorescent fusion protein and show expression in pure C. acetobutylicum using flow cytometry and confocal microscopy. This will allow us to examine the localization of Cac Fd-FAST in co-culture with far-red labeled Clj ptaHaloTag (and Janelia 646 fluorogen) or ptaSNAP-tag (and 647-SiR fluorogen). The massive exchange of the whole proteome between the two organisms in coculture demonstrates that the cells use proteins from both organisms thus exchanging electrons directly. This was further supported by the dramatically reduced H2 production in coculture, which means that the electrons were used to produce alcohols (isopropanol and 2,3 butanediol) by C. ljungdahlii dehydrogenases rather than producing H2 by C. acetobutylicum. We showed evidence for C. ljungdahlii chemotaxis towards CO2 and H2 (as a potential driver and first step to enable heterologous cell fusion) in a novel anaerobic swim assay. We also showed that the movement of C. ljungdahlii towards CO2 can be quantified through qPCR analysis of genome copies that pass through a sterile polycarbonate filter. In addition to this evidence, we identified 2 genes that could be involved in the mechanism for CO2 sensing in C. ljungdahlii, CA (CLJU_c10130) and MeChe (CLJU_c10160). These genes showed a significant fold change in expression when grown in the presence of 80% H2 20% CO2 compared to a N2 and fructose grown control. We have also provided strong evidence to formation of hybrid cells containing DNA from both organisms, and evidence for some persistence of such hybrid cells. We started developing methods (DNA-FISH) to examine the presence of the two different chromosomes in these hybrid cells. We also started the developing high-throughput tools based on constructing transposon insertion libraries in order to start identifying genes and proteins that enable the heterologous cell fusion.

Training Opportunities: Three graduate students and one undergraduate student (Yin Zou) were trained during the execution of this grant (Hannah Streett, Kamil Charubin, John Hill). Kamil Charubin and Hannah Streett completed their PhD thesis. Dr. Gwendoly Gregory also worked on the DNA transfer aspects of the work for 4 months. The students were trained in advanced microbiological and molecular methods of complex consortia, flow cytometry, a broad spectrum of microscopies (optical, fluorescent, TEM, SEM, correlative microscopies). The students also developed strong communication skills from preparing documents and presentations.

Results Dissemination: Streett, H. E., K. M. Kalis and E. T. Papoutsakis (2019). "A Strongly Fluorescing Anaerobic Reporter and Protein-Tagging System for Clostridium Organisms Based on the Fluorescence-Activating and Absorption-Shifting Tag Protein (FAST)." Applied and Environmental Microbiology 85(14): e00622-00619.

Charubin, K., H. Streett and E. T. Papoutsakis (2020). "Development of Strong Anaerobic Fluorescent Reporters for Clostridium acetobutylicum and Clostridium ljungdahlii Using HaloTag and SNAP-tag Proteins." Applied and Environmental Microbiology 86(20): e01271-01220.

Charubin, K., S. Modla, J. L. Caplan and E. T. Papoutsakis (2020). "Interspecies Microbial Fusion and Large-Scale Exchange of Cytoplasmic Proteins and RNA in a Syntrophic Clostridium Coculture." Mbio 11(5): e02030-02020.

Streett, H., K. Charubin and E. T. Papoutsakis (2021). "Anaerobic fluorescent reporters for cell identification, microbial cell biology and high-throughput screening of microbiota and genomic libraries." Curr Opin Biotechnol 71: 151-163.

Charubin, K., G. J. Gregory and E. T. Papoutsakis (2021). "Novel mechanism of plasmid-DNA transfer mediated by heterologous cell fusion in syntrophic coculture of Clostridiumorganisms." bioRxiv: 2021.2012.2015.472834.

Honors and Awards: The PI (Papoutsakis)
1) was elected to the International Academy of Medical & Biological Engineering (2021).
2) was elected to National Academy of Inventors (2021).
3) received the 2020 American Society for Microbiology Award for Applied and Biotechnological Research.
4) Received the 2022 Charles Thom Award (the senior award) of the Society of Industrial Microbiology and Biotechnology (SIMB).
5) Received the 2022 William H. Walker Institute Award (the top award) of the American Institute of Chemical Engineers.

Protocol Activity Status:

Technology Transfer: Nothing to Report

RPPR Final Report
as of 08-Dec-2022

PARTICIPANTS:

Participant Type: PD/PI
Participant: Eleftherios (Terry) Papoutsakis
Person Months Worked: 10.00 **Funding Support:**
Project Contribution:
National Academy Member: Y

Participant Type: Graduate Student (research assistant)
Participant: Kamil Charubin
Person Months Worked: 12.00 **Funding Support:**
Project Contribution:
National Academy Member: N

Participant Type: Graduate Student (research assistant)
Participant: Hannah Streett
Person Months Worked: 15.00 **Funding Support:**
Project Contribution:
National Academy Member: N

Participant Type: Graduate Student (research assistant)
Participant: John Hill
Person Months Worked: 8.00 **Funding Support:**
Project Contribution:
National Academy Member: N

Participant Type: Undergraduate Student
Participant: Yin Zou
Person Months Worked: 4.00 **Funding Support:**
Project Contribution:
National Academy Member: N

Participant Type: Postdoctoral (scholar, fellow or other postdoctoral position)
Participant: Gwendolyn Gregory
Person Months Worked: 4.00 **Funding Support:**
Project Contribution:
National Academy Member: N

ARTICLES:

RPPR Final Report
as of 08-Dec-2022

Publication Type: Journal Article Peer Reviewed: Y **Publication Status:** 1-Published
Journal: Applied and Environmental Microbiology
Publication Identifier Type: DOI Publication Identifier: 10.1128/AEM.00622-19
Volume: 85 Issue: 14 First Page #: e00622-19
Date Submitted: 9/5/22 12:00AM Date Published: 7/1/19 4:00AM
Publication Location: ASM, Washington DC
Article Title: A Strongly Fluorescing Anaerobic Reporter and Protein-Tagging System for
Authors: Hannah E. Streett, Katie M. Kalis, Eleftherios T. Papoutsakis, Maia Kivisaar
Keywords: anaerobic reporter Clostridium acetobutylicum cell biology cell division divisome flow cytometry fusion protein population dynamics protein localization sporulation
Abstract: Visualizing protein localization and characterizing gene expression activity in live Clostridium cells is limited for lack of a real-time, highly fluorescent, oxygen-independent reporter system. Enzymatic reporter systems have been used successfully for many years with Clostridium spp.; however, these assays do not allow for real-time analysis of gene expression activity with flow cytometry or for visualizing protein localization through fusion proteins. Commonly used fluorescent reporter proteins require oxygen for chromophore maturation and cannot be used for most strictly anaerobic Clostridium organisms. Here we show that the fluorescence-activating and absorption-shifting tag protein (FAST), when associated with the fluorogenic ligand 4-hydroxy-3-methylbenzylidene-rhodanine (HMBR; now commercially available) and other commercially available ligands, is highly fluorescent in Clostridium acetobutylicum under anaerobic conditions. Using flow cytometry and a fluorescence microplate rea
Distribution Statement: 1-Approved for public release; distribution is unlimited.
Acknowledged Federal Support: **Y**

Publication Type: Journal Article Peer Reviewed: Y **Publication Status:** 1-Published
Journal: Applied and Environmental Microbiology
Publication Identifier Type: DOI Publication Identifier: 10.1128/AEM.01271-20
Volume: 86 Issue: 20 First Page #: e01271-20
Date Submitted: 9/5/22 12:00AM Date Published: 10/1/20 8:00AM
Publication Location: ASM, Washington DC
Article Title: Development of Strong Anaerobic Fluorescent Reporters for Clostridium acetobutylicum and Clostridium ljungdahlii Using HaloTag and SNAP-tag Proteins
Authors: Kamil Charubin, Hannah Streett, Eleftherios Terry Papoutsakis, Robert M. Kelly
Keywords: Clostridium acetobutylicum, Clostridium ljungdahlii, FAST, HaloTag, SNAP-tag, anaerobic fluorescent reporters, flow cytometry, fluorescent protein, super-resolution microscopy
Abstract: One of the biggest limitations in the study and engineering of anaerobic Clostridium organisms is the lack of strong fluorescent reporters capable of strong and real-time fluorescence. Recently, we developed a strong fluorescent reporter system for Clostridium organisms based on the FAST protein. Here, we report the development of two new strong fluorescent reporter systems for Clostridium organisms based on the HaloTag and SNAP-tag proteins, which produce strong fluorescent signals when covalently bound to fluorogenic ligands. These new fluorescent reporters are orthogonal to the FAST ligands and to each other, allowing for simultaneous labeling and visualization. We used HaloTag and SNAP-tag to label the strictly anaerobic organisms Clostridium acetobutylicum and Clostridium ljungdahlii. We have also identified a new strong promoter for protein expression in C. acetobutylicum, based on the phosphotransacetylase gene (pta) from C. ljungdahlii. Furthermore, the HaloTag and the SNAP-tag
Distribution Statement: 2-Distribution Limited to U.S. Government agencies only; report contains proprietary info
Acknowledged Federal Support: **Y**

RPPR Final Report
as of 08-Dec-2022

Publication Type: Journal Article Peer Reviewed: Y **Publication Status:** 1-Published
Journal: mBio
Publication Identifier Type: DOI Publication Identifier: 10.1128/mBio.02030-20
Volume: 11 Issue: 5 First Page #: e02030-20
Date Submitted: 9/5/22 12:00AM Date Published: 10/1/20 12:00PM
Publication Location: ASM, Washington DC
Article Title: Interspecies Microbial Fusion and Large-Scale Exchange of Cytoplasmic Proteins and RNA in a Syntrophic
Authors: Kamil Charubin, Shannon Modla, Jeffrey L. Caplan, Eleftherios Terry Papoutsakis, Matthew R. Parsek
Keywords: Clostridium ljungdahliiClostridium acetobutylicumsyntrophyheterologous cell fusionhybrid cellsprotein exchangeRNA exchangeanaerobic fluorescent proteinsbacteriahybrid bacteria
Abstract: Microbial syntrophy is universal in nature, profoundly affecting the composition and function of microbiomes. We have recently reported data suggesting direct cell-to-cell interactions leading to electron and material exchange between the two microbes in the syntrophy between Clostridium ljungdahlii and C. acetobutylicum. Here, transmission electron microscopy and electron tomography demonstrated cell wall and membrane fusions between the two organisms, whereby C. ljungdahlii appears to invade C. acetobutylicum pole to pole. Correlative fluorescence transmission electron microscopy demonstrated large-scale exchange of proteins. Flow cytometry analysis captured the extent and dynamic persistence of these interactions. Dividing hybrid cells were identified containing stained proteins from both organisms, thus demonstrating persistence of cells with exchanged cellular components. Fluorescence microscopy and flow cytometry of one species with stained RNA and the other tagged with a fluores
Distribution Statement: 3-Distribution authorized to U.S. Government Agencies and their contractors
Acknowledged Federal Support: **Y**

Publication Type: Journal Article Peer Reviewed: Y **Publication Status:** 1-Published
Journal: Current Opinion in Biotechnology
Publication Identifier Type: DOI Publication Identifier: 10.1016/j.copbio.2021.07.005
Volume: 71 Issue: First Page #: 151
Date Submitted: 9/5/22 12:00AM Date Published: 10/1/21 12:00PM
Publication Location:
Article Title: Anaerobic fluorescent reporters for cell identification, microbial cell biology and high-throughput screening of microbiota and genomic libraries
Authors: Hannah Streett, Kamil Charubin, Eleftherios Terry Papoutsakis
Keywords: GENE-EXPRESSION, CLOSTRIDIUM-PERFRINGENS, SYNTHETIC BIOLOGY, TMP-TAG; PROTEIN; SYSTEM; GFP TECHNOLOGY; PROMOTERS; DIFFICILE
Abstract: The lack of real-time reporters in obligate anaerobes has limited studies in gene expression, promoter characterization, library screening, population dynamics, and cell biology in these organisms. While the use of enzymatic, colorimetric, and luminescent reporters has been reported, the need for reliable anaerobic fluorescent proteins is widely acknowledged. Recently, the fluorescent proteins HaloTag, SNAP-tag and FAST have been established as reliable reporters in Clostridium spp., thus suggesting that these reporters can be adopted widely for many obligate anaerobes. With a multitude of labeling options, these anaerobic fluorescent proteins hold a great potential for screening promoters, terminators, and RBS sites, tracking population dynamics in complex multi-species co-cultures, such as microbiomes, screening libraries, and in cell biology studies of protein localization and interactions using high-resolution microscopy.
Distribution Statement: 3-Distribution authorized to U.S. Government Agencies and their contractors
Acknowledged Federal Support: **Y**

RPPR Final Report
as of 08-Dec-2022

Partners

,

I certify that the information in the report is complete and accurate:
Signature: Eleftherios Papoutsakis
Signature Date: 9/5/22 5:51PM

2022 Final Progress Report

ARO Proposal Number: 74827-LS, Agreement Number: W911NF-19-1-0274: Probing direct cell-to-cell exchange of matter in a *Clostridium* syntrophic co-culture

Reporting Period: 5/7/2019 to 7/31/2022

E. T. Papoutsakis (PI), Univ. of Delaware

1. Foreword: Not needed.

2. Table of Contents:

3. List of Appendixes: No Appendixes.

4. Statement of problem studied. The goal of this ARO project is to dissect at the cellular a binary *Clostridium* syntrophic co-culture that exhibits unusual and previously unreported phenomena of cell fusion and direct exchange of matter between the two microbes, based on data developed under the support of an ARO STIR grant. The syntrophic system is made up of *Clostridium acetobutylicum* (***Cac***), which converts simple and complex carbohydrates into solvents and carboxylates, and the acetogen *C. ljungdahlii* (***Clj***) which fixes CO_2 (**Fig. 1**). Direct cell-to-cell interactions and material exchange among the two microbes enabled unforeseen metabolic rearrangements. Evidence for direct cell-to-cell interactions was provided using metabolic analysis, fluorescence microscopy (**FM**) and electron microscopies (**TEM** & **SEM**). This includes strong evidence for cell-wall and membrane fusion events and exchange of small molecules, reducing equivalents (electrons) and macromolecules. Here we will test hypotheses aiming to dissect these novel interactions using correlative FM/TEM/SEM and immunogold and/or related nanogold-based electron microscopies to detail the exchange of macromolecules. We will also probe possible direct transfer of nucleic acids (RNA and plasmid DNA) from *Cac* to *Clj*. We will use genetic and culture modifications to identify the mechanism by which *Cac* transfers reducing equivalent ("electrons") to *Clj*: if through direct transport of H_2 or by direct transport of electron-carrier proteins or by generating an artificial interspecies electron-transport chain. Cellular-level understanding of this syntrophy, as proposed here, could lead to many fundamental and practical findings, with applications in environmental sustainability, remediation, the study of natural and synthetic ecosystems and microbiomes, and how they can be used to produce chemicals and fuels from renewable biomass and waste materials, including CO_2, H_2 and syngas that can be generated from various sources (1). Such applications are of interest to ARO as impacting defense-related operations. This grant will support graduate students working in the PI's lab.

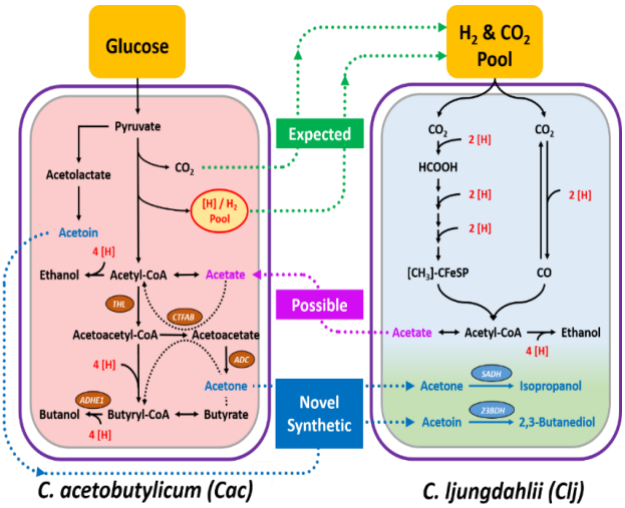

Fig. 1. Syntrophic interactions in the *Cac-Clj* co-culture. *Cac* consumes glucose to produce solvents releasing CO_2 & H_2. *Clj* utilizes CO_2 & H_2 through the Wood-Ljungdahl pathway (WLP) for survival producing acetate and ethanol. In the co-culture, acetone and acetoin produced by *Cac* are reduced by

5. Summary of the most important results

I. Design and expression of a new HaloTag fluorescent protein for *C. acetobutylicum* (*Cac*) and *C. ljungdahlii* (*Clj*). In order to fluorescently visualize both organisms composing our synthetic Cac-Clj co-culture we needed another fluorescent reporter protein. The 2nd fluorescent reporter had to be orthogonal to the previously developed FAST fluorescent reporter (2) in terms of ligand binding (to ensure FAST ligands to no interact with the new protein) and fluorescence wavelength (new reporter must produce fluorescent

signal orthogonal to the green fluorescence produced by FAST and HMBR ligand). Therefore, we used the HaloTag® protein which is capable covalently binding to a variety of fluorescent ligands(3, 4) and uses reactive chloroalkane linker chemistry (5) to bind its ligands, which is orthogonal to FAST. To express the HaloTag protein in *Cac* and *Clj* we created the p100ptaHalo expression plasmid which can be expressed in both organisms. The backbone of the p100ptaHalo was the modified pSOS95 clostridia-*E. coli* shuttle vector (Amp^R, MLS^R, *thl* promoter, rho-independent terminator, ColE1 ori, repB ori)(6). The repB origin of replication is of importance as it is compatible with both *Cac* and *Clj*. The HaloTag® was codon-optimized for expression in clostridia and synthesized. To express the HaloTag in both *Cac* and *Clj* we used the promoter from phosphotransacetylase (*pta*) gene native to *Clj* (P_{pta})(6), and an ribosome-binding sequence (RBS) used previously for expression of heterologous proteins in *Clj* (7). The plasmid was electro-transformed into *Cac* and *Clj* according to previously reported methods (6, 8). We have successfully expressed the HaloTag protein in *Cac* and *Clj* and successfully labeled it with two fluorescent ligands (**Fig. 2**). As shown in **Fig. 2B** and **Fig. 2E**, the Halo-Tag showed strong orange fluorescence in both *Clj* and *Cac* when labeled with the TMR Direct ligand (λ_{em} = 578 nm), when measured with flow cytometer. In comparison, the wild-type cells did not show any fluorescence when labeled with the same ligand (**Fig. 2A & Fig. 2E**). Similarly, both *Clj*-Halo and *Cac*-Halo strain were successfully labeled with the far-red Janelia®646 ligand and visualized using super-resolution confocal microscopy (**Fig. 2C & Fig. 2G**).

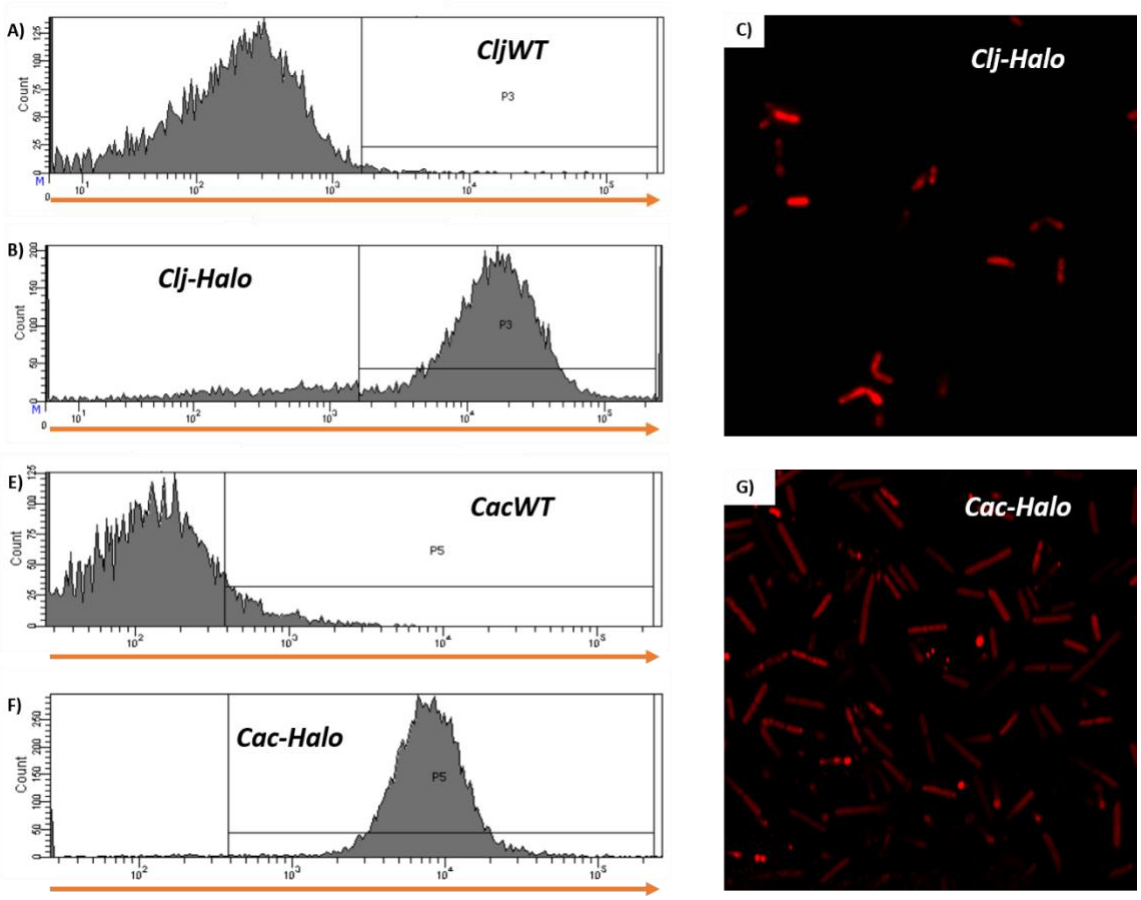

Fig. 2. Fluorescent labeling of **A)** wild-type *Clj*, **B)** *Clj-Halo*, **E)** wild-type *Cac*, and **F)** *Cac-Halo* strains with the HaloTag® TMR Direct™ ligand (λ_{em} = 578 nm, orange). The fluorescence was measured with the flow cytometer (see Methods). Wild-type *Clj* and *Cac* did not show any fluorescence after labeling with the HaloTag®-specific ligand **(A & E)**. In comparison the *Clj-Halo* and *Cac-Halo* strains (plasmid p100ptaHalo) showed high intensity orange fluorescence when labeled with the same TMR Direct™ ligand **(B & F)**. Super-resolution fluorescence imaging of the **C)** *Clj-Halo* strain and **G)** *Cac-Halo* labeled with the Janelia Fluor® 664 nm, far red). The *Clj*-Halo cells showed strong far-red fluorescence under the microscope.

II. Cell-to-cell fusion events facilitate the exchange of whole-cell proteome between *C. acetobutylicum* and *C. ljungdahlii* in the co-culture. We have previously observed that *Cac* and *Clj* physically interact under the co-culture conditions which facilitates the exchange of small molecules (notably acetone and acetoin)(9). Could this interaction also facilitate the exchange of other cellular material such as protein? To test whether both organisms can exchange protein, we co-cultured the *Cac*-FAST strain (which fluoresces green, λ_{em} = 541 nm) with wild-type *Clj* which was fluorescently labeled with the CellTracker Deep Red dye (λ_{em} = 660 nm). The Deep Red dye can freely pass through the cell membrane. Once inside of the cell, its active succinimidyl ester reactive group reacts with amine groups of intracellular proteins, rendering the dye membrane impermeant and thus is retained in living cells through several generations, whereby the dye is transferred to daughter cells but not adjacent cells in a population (10). Control experiments confirmed that this was indeed the case. *Cac*-FAST and red-labeled *Clj* with CellTracker Deep Red were co-cultured and samples were used for correlative confocal/TEM microscopy. First, confocal microscopy was used to identify *Cac*-*Clj* clusters in the sample and visualize the localization of fluorescent proteins (FAST protein in *Cac*, and all intracellular proteins in *Clj*). In the *Cac*-*Clj* fusion cluster shown in **Figs. 3A-E**, the red fluorescence signal (CellTracker Deep Red tagged *Clj* proteins) was stronger in the top cell (**Fig. 3A**) and appeared to diffuse in the downward direction into the bottom cell. The green fluorescent signal (FAST protein) showed the reverse trend, where the bottom cell had a stronger green fluorescence (**Fig. 3B**). Based on the intensity of red and green fluorescence the top cell is arguably red-labeled *Clj*, while the bottom cell is the green-labeled *Cac*-FAST cell. The identity of each cell was confirmed using correlative TEM imaging (see Methods). TEM confirmed that the top cell was a "homogenous" *Clj* cell, while the bottom cell was a differentiating *Cac*-FAST cell (**Fig. 3D**). Their peptidoglycan walls appear fused at the poles (**Fig. 3E**). Furthermore, the differential red and green fluorescence intensities indicate the exchange of protein material between the two organisms. The intensity of the red signal appeared to decrease from approximately the halfway point of *Clj* cell, through the fusion site, and toward the bottom of the *Cac* cell (**Fig. 3A**). This suggests intracellular *Clj* proteins diffused into the *Cac* cytoplasm. Similarly, the intensity of the green signal was stronger in the bottom *Cac*-FAST cell and decreased from the fusion site toward the top of the *Clj* cell (**Fig. 3B).** To further pursue the protein exchange between *Cac*-FAST and red-labeled *Clj* cells (**Figs. 3A-J**), we carried out co-culture experiments with different strains of *Cac* and *Clj*. Here we used the *Cac*-ZapA-FAST strain, which expresses a fusion protein of the fluorescent FAST protein and the ZapA protein involved in cell division in *Cac* and other clostridia (11). Instead of fluorescently labeling *Clj* using the protein binding CellTracker Deep Red dye, we used the *Clj*-Halo (**Fig. 2A-C**). We used Janelia Fluor646® to label the *Clj*-Halo strain, which produces far-red fluorescence orthogonal to the green fluorescence produced by FAST. The *Clj*-Halo strain was co-cultured with the *Cac*-ZapA-FAST strain and imaged after 20 hrs of co-culture growth. **Figs. 3K-M** show a cell fusion event between the two strains similar to **Figs. 3A-E**. Here the top cell had strong red fluorescence, and was identified as a *Clj*-Halo cell, while the bottom cell had strong green fluorescence and therefore was identified as a *Cac*-ZapA-FAST cell. The red labeled HaloTag® peptide diffused downward into the *Cac*-ZapA-FAST cell, while the green ZapA-FAST fusion protein diffused upwards into the *Clj*-Halo cell.

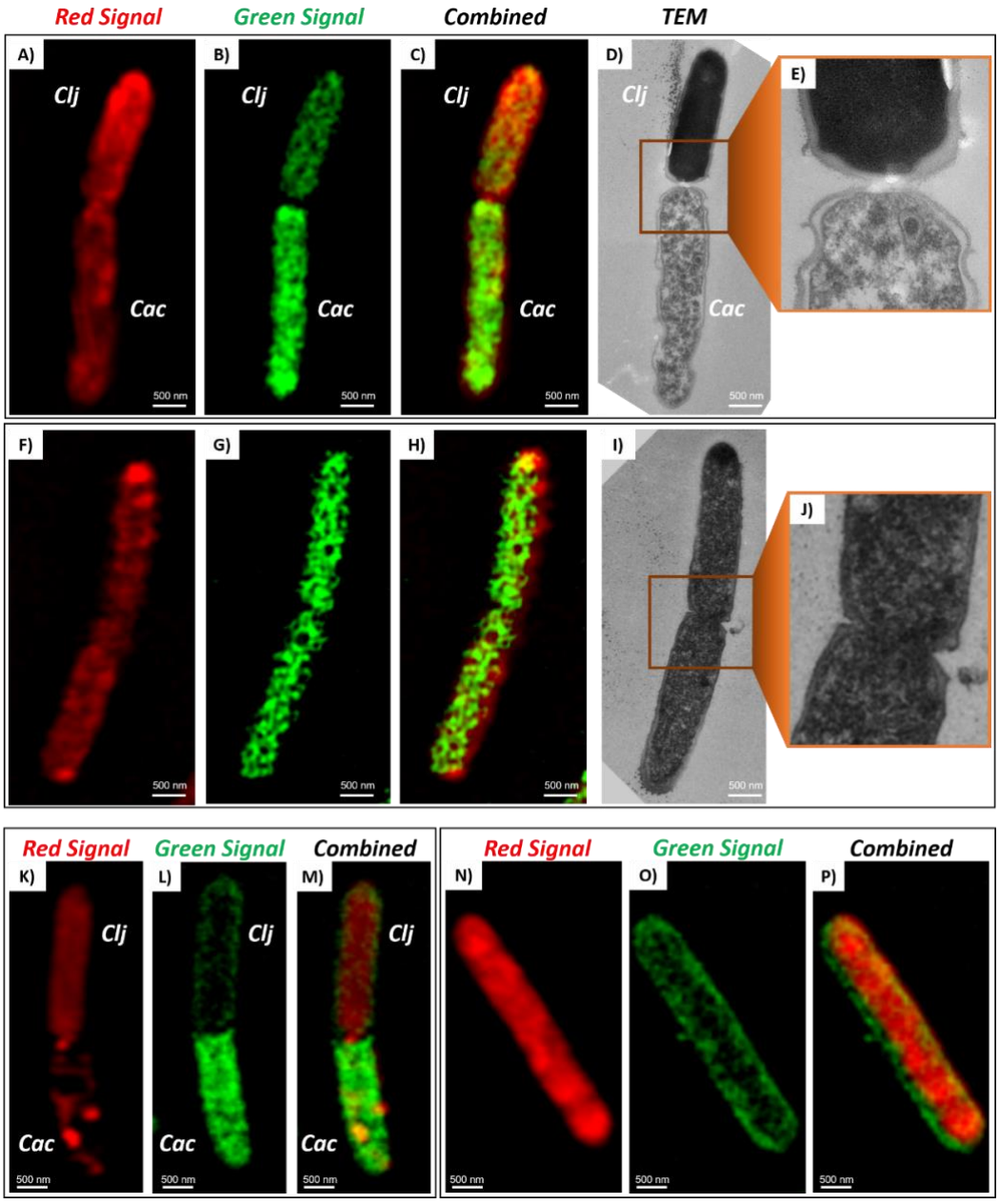

Fig. 3. Four *Cac*-*Clj* clusters captured using correlative fluorescence & TEM microscopy. The red signal was produced by the CellTracker™ Deep Red dye bound to *Clj*'s proteins **(A-H)**, and Janelia 646 ligand bound to the HaloTag in *Clj*-Halo **(K-P)**. The green signal was produced by the HMBR ligand bound to FAST **(A-H)**, and ZapA-FAST fusion protein **(K-P)** in *Cac* strains. The fluorescent images were captured in the Z-stack mode using super-resolution microscopy. Clusters **(A-E)** and **(F-)** were also imaged using TEM (see Methods for details) to visualize each cell's cytoplasm **(D, I)**. The top panels show a cell fusion event between red-labeled *Clj* and green *Cac*-FAST. Panel **E)** shows a close up of the interaction between the red *Clj* and green *Cac* at the poles. Middle panels show a *Cac*-*Clj* hybrid cell undergoing cell division after acquiring both red and green fluorescent materials. Panel **J)** shows the close up of the cell division site. The same type of interaction was found in the co-culture between *Cac*-ZapA-FAST and *Clj*-Halo **(K-P)**. The cluster **(K-M)** shows a fusion event between *Clj*-Halo and *Cac*-ZapA-FAST. The strains were identified based on the strength of each

III. Cell fusion between *C. acetobutylicum* and *C. ljungdahlii* results in exchange of cellular RNA. As shown above, the cell fusion events between *Cac* and *Clj* facilitated the exchange of whole-cell proteome between both organisms. Since both organisms were exchanging large molecules like protein, it was likely they exchanged other cellular material such as RNA. To test for RNA exchange, we labeled wild-type *Clj* with the SYTO™ RNASelect™ dye, which fluoresces green only when bound to RNA

molecules. *Clj* cells with labeled RNA were co-cultured with the *Cac*-Halo strain expressed the HaloTag protein (**Fig. 2**). Starting at 4 hrs of co-culture we observed cell fusion events similar to those seen in **Fig. 3**, where red Cac-*Halo* was fused with a *Clj* cell containing labeled RNA (**Figs. 4A-C**). This cluster in particular is interesting since the red *Cac*-Halo acquired some of *Clj*'s green RNA during the fusion, while the *Clj* cell did not acquire any red protein material from *Cac*-Halo. Therefore, the exchange of whole-cell RNA must occur at a faster rate and to a greater degree compared to protein exchange. In comparison, the cell fusion cluster from 20 hrs of co-culture (**Figs. 4M-O)** shows the exchange of both RNA and protein later on in the co-culture. Here, the top cell is the *Clj* containing strong green signal (labeled RNA) and weaker red signal coming from red HaloTag protein acquired from *Cac*-Halo. Similarly, the bottom cells must be a *Cac*-Halo cells since it contains strong red signal (HaloTag), and weaker green signal produced by green RNA acquired from *Clj* (top cell). This is consistent with flow cytometry time course data where double-positive cells were observed only after 2 hrs of co-culture, and the double-positive fraction reached 51.9% by 27 hrs of co-culture (**Suppl. Fig. 9**). Furthermore, single hybrid cells containing green RNA material and red protein material were observed at throughout the co-culture at 4 hrs (**Figs. 4D-F**), 9 hrs (**Figs. 4J-L**) and 20 hrs (**Figs. 4P-R**). The cells shown in **Figs. 4P-R** from a 20 hrs sample is of particular interest as it shows a Cac-*Halo* cell in the clostridial form (which is part of its sporulation mechanism (12)) containing the red HaloTag and the green RNA acquired from *Clj*. Thus, *Cac* that acquired foreign RNA from *Clj* was still able to function and go through its normal sporulation process.

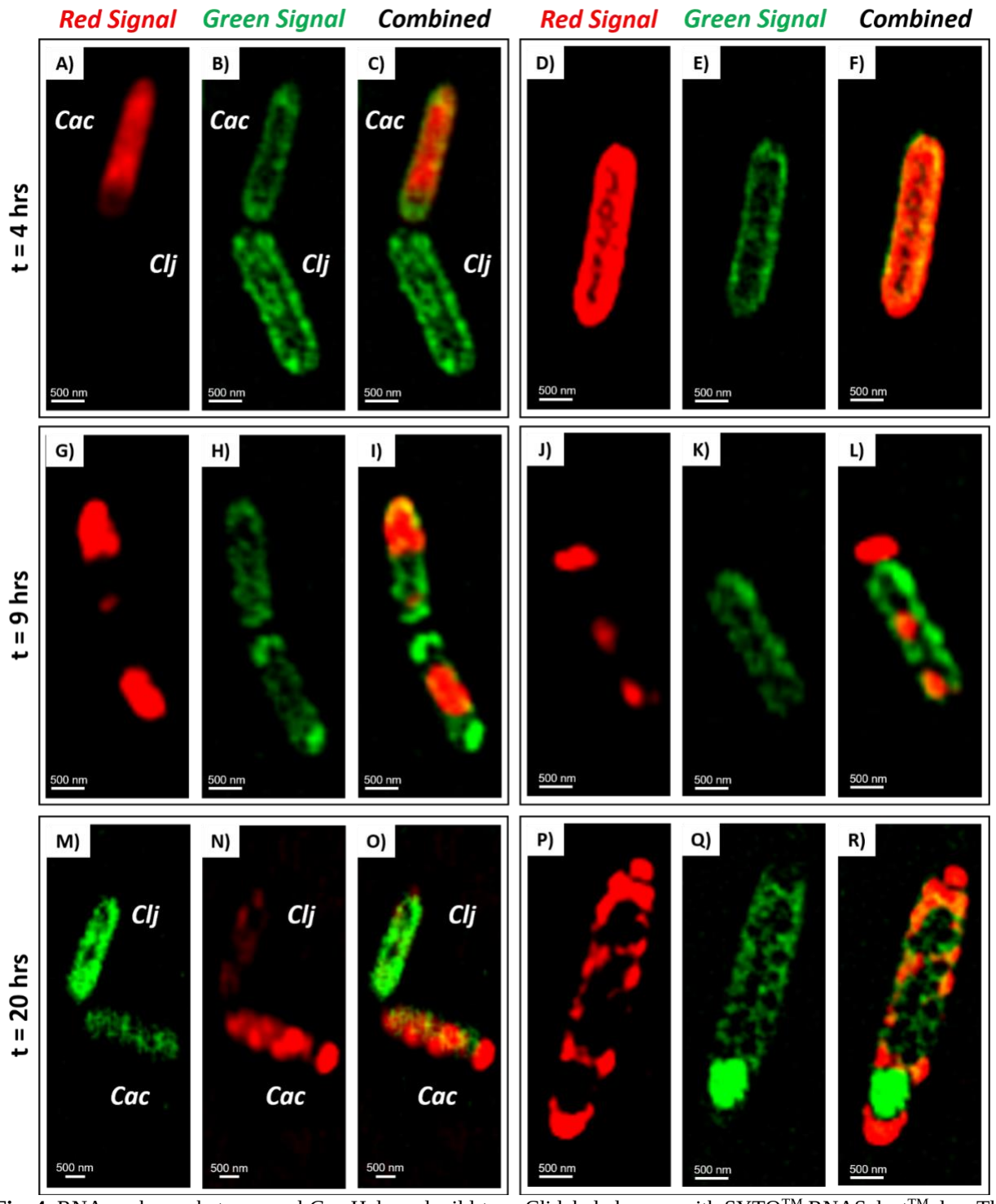

Fig. 4. RNA exchange between red *Cac*-Halo and wild-type Clj labeled green with SYTO™ RNASelect™ dye. The red signal was produced by the Janelia 646 ligand, while the green was produced by the RNASelect™ bound to *Clj*'s whole-cell RNA. Thus, the red signal indicates presence of protein (HaloTag) while the green color indicates. The images were collected in the Z-stack mode using a super-resolution confocal microscope. Two cell clusters are shown at 4 hrs, 9 hrs, and 20 hrs of the co-culture. The presence of two-cell double-positive clusters early on in the co-culture indicates whole-cell RNA is freely exchanged between both organisms under co-culture conditions.

IV. SNAP-tag represents an orthogonal fluorescent reporter systems to use with FAST and HaloTag in labeling of *Clostridium* co-cultures. To observe the direct transfer of proteins between *Clostridium* species, other orthogonal fluorescent reporter systems are needed tag multiple proteins of interest. Our lab has successfully used FAST and Halo-tag to label both *C. acetobutylicum* and *C. ljungdahlii* and we have designed an additional orthogonal fluorescent system for *Clostridium spp*. using the SNAP-tag. SNAP-tag is a mutant DNA repair protein O6-alkylguanine-DNAalkyltransferase transfers the alkyl group of the substrate permanently to a cysteine residue (13). SNAP-tag irreversibly binds benzylguanine derivatives like SNAP-Cell 647-SiR and benzylchloropyrimidine derivatives like SNAP-Cell 505-Star and SNAP-Cell TMR-Star. Halo-tag and SNAP-tag used in addition to FAST results in 3 different orthogonal labeling methods for tagging *Clostridium spp*. The thl^{sup} promoter used previously in *C. acetobutylicum* when characterizing FAST as a fluorescent reporter (14) and also shows higher fluorescence intensity compared to WT *C. acetobutylicum* when incubated with TMR-Star fluorescent ligand when expressing codon optimized SNAP-tag (**Fig. 5A-B**). The *thl* promoter resulted in 8.4% of labeled cells after 7 hours of culture and increased up to 21.5% after 35 hours, while the thl^{sup} promoter resulted in stable expression of the SNAP-tag resulting in 47.2% of labeled cells throughout the 35 hours of growth. This is consistent with what we have shown previously using the anaerobic FAST fluorescent tag (2). Cac thl^{sup}SNAP-tag also shows brightly fluorescent cells using confocal microscopy (**Fig 5C**). Cac thl^{sup}SNAP-tag shows significantly higher mean fluorescence intensity (MFI) compared to WT C. acetobutylicum when incubated with the orange fluorescent ligand SNAP-Cell TMR-Star (**Fig 5D**).

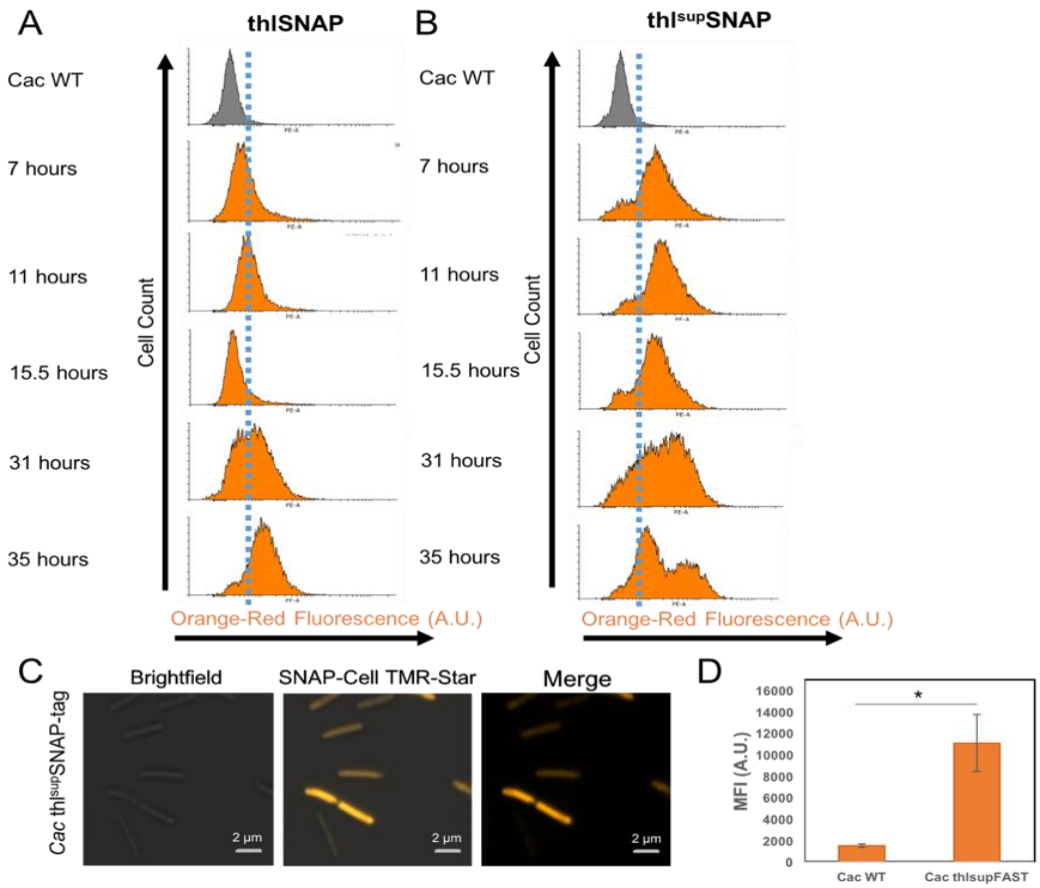

Fig. 5. *C. acetobutylicum* thlSNAP-tag and thl^{sup}SNAP-tag show fluorescence consistent with previously shown fluorescence using thiolase promoters. A) *C. acetobutylicum* thlSNAP-tag shows fluorescence brighter than WT *C. acetobutylicum* after 7, 11, 15.5, 31, and 35 hours of growth. B) *C. acetobutylicum* thl^{sup}SNAP-tag shows fluorescence brighter than WT *C. acetobutylicum* after 7, 11, 15.5, 31, and 35 hours of growth. C) *C. acetobutylicum* thl^{sup}SNAP-tag shows bright fluorescence when incubated with orange-red SNAP-Cell TMR-Star after ~8 hours of growth. D) *C. acetobutylicum* thl^{sup}SNAP-tag shows higher Geometric Mean Fluorescence Intensity (MFI) compared to WT *C. acetobutylicum* when incubated with orange-red SNAP-Cell TMR-Star after ~8 hours of growth. Error bars represent SD. *p<0.05.

Because the *thl^{sup}* promoter resulted in the higher expression of SNAP-tag in *C. acetobutylicum*, we used the same SNAP-tag operon (and replaced the repL with repB ori in the backbone) in *C. ljungdahlii* to make the *Clj*-thl^{sup}SNAP strain. Clj thl^{sup}SNAP also shows higher fluorescence intensity compared to WT *C. ljungdahlii* incubated with TMR-Star (**Fig 6A**). We also tested the pta promoter for expressing SNAP-tag and *Clj* ptaSNAP-tag showed brighter orange fluorescence (**Fig 6A**) and more brightly fluorescent cells than *Clj* thl^{sup}SNAP-tag (**Fig 6B**). However, SNAP-tag expressed in *Clj* with the RepB replisome with both the pta promoter and the thl^{sup} promoter does not show as dramatic of a shift in fluorescence intensity compared to WT as the pta promoter appears to with the Halo-tag (**Fig 2**). To have orthogonal fluorescent reporters for multiple *Clostridium spp*. it is crucial for no cross reactivity between fluorescent reporters.

When paired with a far-red ligand, both Halo-tag and SNAP-tag (Janelia 646 and 647-SiR respectively) show distinct populations from FAST paired with a green fluorescent ligand (HMBR and ^{TF}Lime) when co-incubated (**Fig. 7**). When *Clj* ptaHalo-tag and *Cac* thl^{sup}FAST co-culture is incubated with both Janelia 646 and HMBR, two separate populations are shown with flow cytometry using FITC (green) and APC (far-red) (**Fig. 7A**). Additionally, *Cac* thl^{sup}SNAP and *Cac* thl^{sup}FAST incubated with 647-SiR

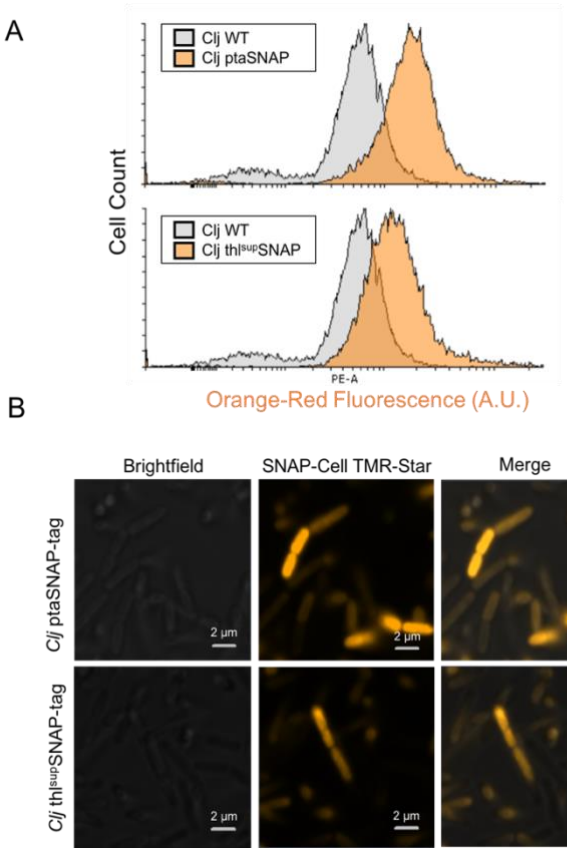

Fig. 6. *C. acetobutylicum* and *C. ljungdahlii* labeled with SNAP-tag using *C. acetobutylicum* thl^{sup} promoter. *C. acetobutylicum* labeled with SNAP-tag expressed using the *Cac* thl^{sup} promoter and the red-orange fluorescent ligand, TMR-Star (left confocal and top histogram). *C. ljungdahlii* labeled with SNAP-tag expressed using the *C. acetobutylicum* thl^{sup} promoter and labeled using the red-orange fluorescent ligand, TMR-Star (right confocal and bottom histogram).

divisome protein ZapA, CLJU_c34400, which has not been previously characterized. To express *Cac* ZapA-FAST in *C. ljungdahlii* the same pta promoter and RBS used with Halo-tag in p100ptaHalo with the RepB replisome was used. *C. ljungdahlii* ptaZapA-FAST shows bright fluorescence using flow cytometry compared to WT *C. ljungdahlii* when incubated with HMBR (**Fig. 8A**). Confocal microscopy shows that *C. acetobutylicum* ZapA-FAST localizes at a single pole in *C. ljungdahlii* cells (**Fig 8B**). This provides an indication of where ZapA-FAST will localize if ZapA-FAST plasmid can be transmitted between species in co-culture and expressed by *C. ljungdahlii*.

and HMBR show separate populations using the same FITC and APC filters (**Fig. 7B**). The overlapping green and far-red signal populations is less than 1%, showing distinct and orthogonal labeling strategies of both HaloTag and SNAP-tag with FAST.

V. *C. ljungdahlii* ptaZapA-FAST fluorescent fusion protein shows localization at single pole in pure culture. While the transfer of cellular *Cac* ZapA-FAST protein has been shown in co-culture (**Fig 3**), we wanted to determine the phenotype of *Clj* cells expressing Cac ZapA-FAST and observe localization of overexpressed *C. acetobutylicum* ZapA-FAST in pure *C. ljungdahlii* culture. Natively, *C. ljungdahlii* expresses a predicted homolog the predicted *C. acetobutylicum* cell

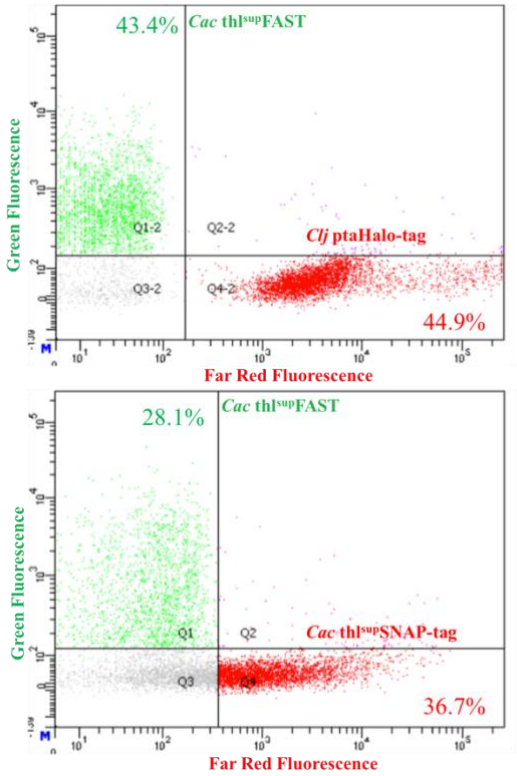

Fig. 7 Separation of Halo-tag *Clj* (top) SNAP-tag *Cac* (bottom) from *Cac* thl^{sup}FAST after co-incubation of each respective ligands.

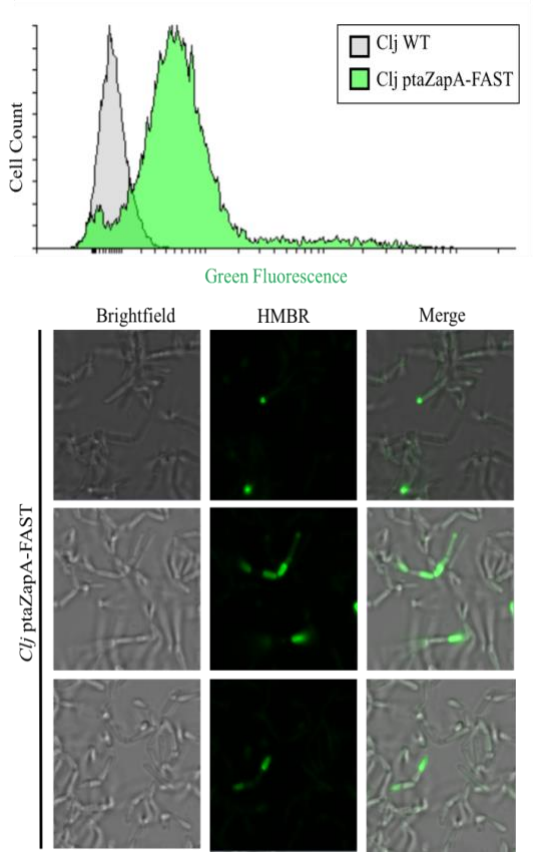

Fig. 8. *C. ljungdahlii* expressing *C. aceobutylicum* ZapA-FAST fusion protein using the native *C. ljungdahlii* pta promoter. *C. ljungdahlii* ptaZapA-FAST shows higher fluorescence intensity compared to WT *C. ljungdahlii* (top). Confocal images of overexpressed *C. acetobutylicum* ZapA-FAST appears to localize at a single pole of

VI. Successful design of *C. acetobutylicum* ferredoxin fusion protein with FAST (thlFd-FAST).

In addition to utilizing ZapA-FAST to view transfer of plasmid and protein, we have designed an additional fluorescent fusion protein to test plasmid and protein transfer using *C. acetobutylicum* ferredoxin (CAC0303). *Cac* Fd has been shown to be the major ferredoxin expressed in *C. acetobutylicum* (15, 16) and has been suggested the *in vivo* application of this ferredoxin is to channel electrons to HydA1 (15), the main hydrogen producing hydrogenase in *C. acetobutylicum*. The fusion protein was constructed as the *C. acetobutylicum* ZapA-FAST was previously (14) using the native thl promoter and a flexible fusion protein linker. We will use this thlFd-FAST fusion to observe the potential localization of ferredoxin during cell-to-cell interactions in co-culture. First, to examine potential localization of ferredoxin in pure *C. acetobutylicum* thlFd-FAST, we observed with both flow cytometry and confocal microscopy. Flow cytometry showed brightly fluorescent cells expressing the Fd-FAST fusion protein and showed higher fluorescence intensity when compared to WT *C. ljungdahlii* (**Fig. 9**). Using confocal microscopy, Fd-FAST appears to localize in small areas of certain cells, shown by red arrows, which presumably shows Fd-FAST interacting with native proteins in *C. acetobutylicum*.

VII. Evidence for transfer of plasmid DNA from *C. ljungdahlii* (*Clj*) to *C. acetobutylicum* (*Cac*), facilitated by the unique cell fusion events that occur in the co-culture. The syntrophic co-culture system discovered in this work provides evidence for a new, and never-previously described mechanism for the horizontal gene transfer between bacteria. Here, the exchange of plasmid, and possibly genomic DNA has occurred through the cell-to-cell fusion that takes place in the syntrophic co-culture of *C. acetobutylicum* (*Cac*) and *C. ljungdahlii* (*Clj*) and has been documented previously (17). In the co-culture, the cell-to-cell fusion and the formation of hybrid bacterial cells may have facilitated the exchange of DNA between these two unique organisms. As detailed below, plasmid DNA (p100ptaHalo) was successfully transferred from the *Clj*-ptaHalo strain expressing the HaloTag protein (18), to the wild-type *Cac* in the co-culture of the two organisms. The gene transfer between these two organisms could not have occurred through the natural competency route, where *Cac* picked up the plasmid DNA from any lysed *Clj*-ptaHalo, for two reasons. First, there is no evidence that either *Cac* or *Clj* have the ability to become naturally competent (19, 20). Second, the RM methylation system of *Clj* is not compatible with that of *Cac*, which prevents the transformation with *Clj*-methylated plasmids into *Cac*, as described later. Thus, the observed DNA exchange must have occurred through the unique cell-to-cell fusion observed in the co-culture of the two organisms. Since neither organism is known to possess any conjugation machinery, the cell-to-cell fusion and formation of hybrid bacterial cells that occurs in the co-culture of these two organisms is likely to be a never-previously seen mechanism of horizontal gene transfer.

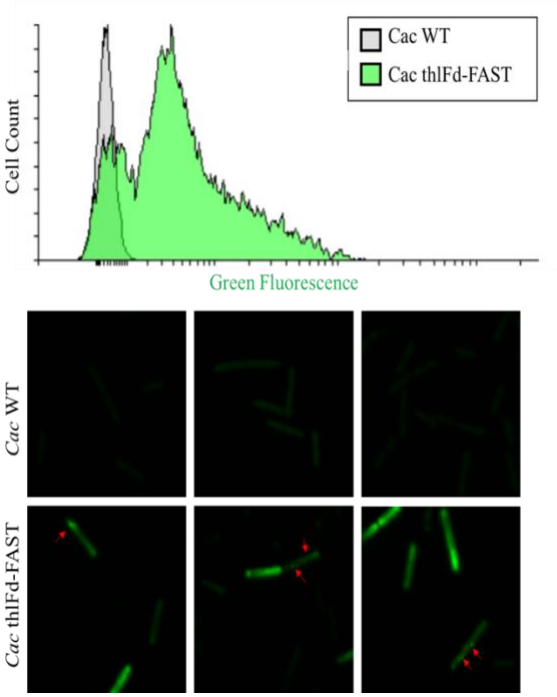

Fig. 9 *C. acetobutylicum* expressing thlFd-FAST fusion protein fluorescence compared to WT *C. acetobutylicum. C. acetobutylicum* thlFd-FAST shows higher fluorescence intensity compared to WT using flow cytometry (top) and thlFd-FAST shows small localizations of fluorescence in some

VIII. Design of the selection process for isolating *Cac* cells which acquired plasmid DNA from *Clj*-ptaHalo under co-culture conditions. To determine if DNA can be transferred between *Clj* and *Cac* under co-culture conditions, four co-cultures (biological replicates) of *Clj*-ptaHalo strain (carrying p100ptaHalo plasmid compatible with both organisms) and the wild-type *Cac* were performed. After 24 hrs of growth, co-culture samples were collected for selection in order to isolate any *Cac* that may have acquired the p100ptaHalo plasmid (carrying the HaloTag gene and the erythromycin resistance gene, Erm^R) from the *Clj*-ptaHalo strain. The selection was done in liquid medium during the first two steps, followed by selection on and solid selection plates. The liquid selection was done in Turbo CGM, containing 80 g/L of glucose (*Cac* specific substrate) and no fructose (*Clj* specific substrate), supplemented with 100 µg/mL of erythromycin. The liquid selection cultures were done in unsealed 100 mL bottles in the anaerobic chamber with no extra

H_2/CO_2 gas (*Clj* specific substrate). The plate selection was done on 2xYTG plates, containing 5 g/L of glucose, no fructose, and 100 µg/mL of erythromycin. Therefore, in the liquid and solid selection, the presence of only high glucose concentration (*Cac* substrate), and no fructose, nor concentrated gas sources present (*Clj* substrates), was expected to enrich the original co-cultures samples in *Cac* cells, while eliminating *Clj*-ptaHalo over time. The selection media also contained the antibiotic erythromycin (100 µg/mL) in order to eliminate wild-type *Cac* cells during the selection process, and over time isolate only *Cac* cells that acquired the plasmid DNA (p100ptaHalo) in the co-culture. The isolated strains are defined from this point on as *Cac*-X.#, where 'X' represents the different starting co-cultures, while the '#' represents the specific selection stage (passage), as shown in **Figure 1**.

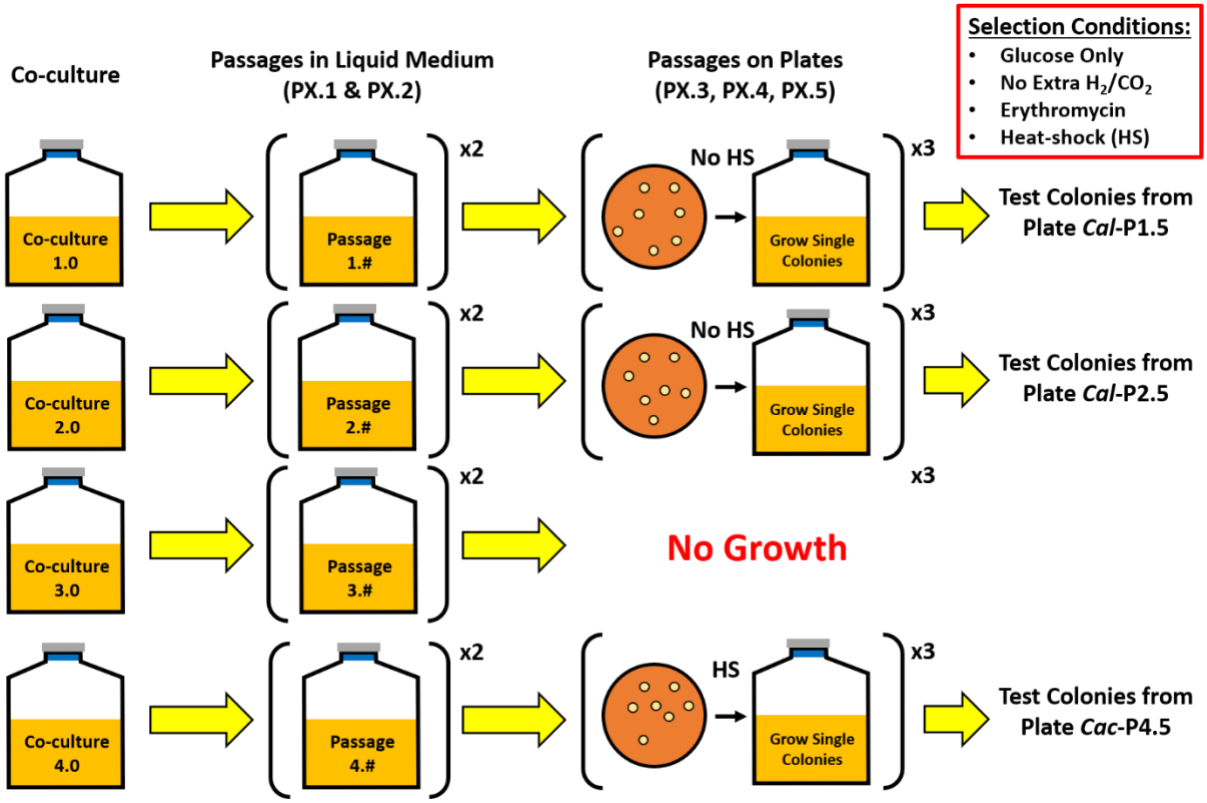

Figure 10. The summary of the selection procedure for isolating *Cac*-PX.# strains, which acquired the plasmid DNA from *Clj*-ptaHalo in the co-culture. The selection started with 4 co-cultures. In the first two selection passages (PX.1, and PX.2) co-culture samples were incubated in selective liquid medium. At the passage PX.3, cells were plated on selective plates to generate and isolate single colonies of *Cac*-X.# strains, which have acquired the plasmid DNA. The selection line *Cac*-P3.2 did not survive on plates and was abandoned. Selection lines *Cac*-1.3 and *Cac*-2.3 (and all subsequent passages) could not survive the heat-shock, indicating the lack of sporulation genes, and were grown without heat-shock selection for analysis. The selection passage line *Cac*-P4.3 (and all subsequent passages) survived the heat-shock, thus showing a phenotype consistent with wild-type *Cac*.

To start the selection process, 5 mL samples from each co-culture were washed in Turbo CGM medium (80 g/L of glucose only, no fructose) and transferred to 25 mL of the liquid selection medium. The co-culture samples were washed to remove any fructose left over from the co-culture growth medium. This was the 1st selection passage PX.1 (Figure 10). After 24 hrs of growth, 5 mL samples from each PX.1 culture were collected, washed, and transferred to fresh 25 mL of the

liquid selection medium again (passage PX.2) to further enrich the passaged cultures for plasmid-containing *Cac* cells. After 24 hrs of incubation, samples from passages PX.2 were steaked onto 2xYTG selection plates (PX.3) to begin isolating and testing single colonies. Plating on the 2xYTG selection plates was expected to further eliminate any pure *Clj*-ptaHalo cells from the selection samples, since *Clj* cells do not develop colonies on plate surface, and instead have to be imbedded within the agar to grow (6, 16). The selection plates (PX.3) developed colonies after 2 days of incubation at 37°C, except the selection plate P3.3 which did not develop any colonies (Figure 10). Thus, the P3.# selection line was abandoned at that point. Multiple colonies (8-10) were picked from each successful selection plate (P1.3, P2.3, & P4.3) and were cultured in the liquid selection medium (80 g/L glucose with 100 µg/mL erythromycin). Half of the selected colonies were heat-shocked at 80°C for 10 minutes (per standard *Cac* culture techniques) to check whether the colonies from the selection plates were still able to sporulate. Colonies from plates P1.3 and P2.3 did not survive the heat-shock selection, but were able to grow in the liquid selection medium, while colonies from the plate P4.3 survived the heat-shock and grew in the liquid selection medium. All colonies that grew in the liquid selection medium were then streaked again on the 2xYTG selection plate (passage PX.4), and the process was repeated one more time (passages PX.5) to further enrich each selection strains (P1.#, P2.#, and P4.#) for *Cac* cells resistant to erythromycin. Finally, colonies from plates P1.5, P2.5, and P4.5 were grown in the liquid selection medium, and analyzed using microscopy, flow-cytometry, HPLC, and PCR assays to determine whether the plasmid DNA (and any genomic DNA) were transferred from *Clj*-ptaHalo to the wild-type *Cac* cells during co-culture.

Table 1. The phenotype checklist of the parent strains used for the starting co-culture (Clj-ptaHalo and wild-type Cac), the expected phenotype of Cac cells which acquired the plasmid DNA and the observed phenotype in the isolate.

Characteristic	***Clj*-ptaHalo**	**Wild-type *Cac***	***Cac*-ptaHalo (p100ptaHalo)**	***Cac*-P4.5 Strain**	
Heat-shock survival	**No**	**Yes**	**Yes**	**Yes**	***Cac* Specific**
Growth on glucose only	**No**	**Yes**	**Yes**	**Yes**	
Growth on plates	**No**	**Yes**	**Yes**	**Yes**	
Prod. of butanol, acetone, acetoin	**No**	**Yes**	**Yes**	**Yes**	
Growth on erythromycin	**Yes**	**No**	**Yes**	**Yes**	**Plasmid Specific**
HaloTag fluorescence	**Yes**	**No**	**Yes**	**No**	
Production of isopropanol	**No**	**No**	**No**	**No**	**Co-culture Specific**

IX. Successful transfer of plasmid DNA from *Clj*-ptaHalo strain to the wild-type *Cac* in the co-culture. Of the four starting co-culture selection lines (Figure 10), only the *Cac*-P4.5 strain showed almost the full expected phenotype of *Cac* cells that acquired the plasmid DNA

(p100ptaHalo) from *Clj-pta*Halo strain. The phenotype of all cells was determined based on seven characteristics:

1) Survival of the heat-shock selection (*Cac* phenotype only)
2) Growth on the plate surface (*Cac* phenotype only)
3) Growth on glucose only (*Cac* phenotype only)
4) Production of butanol (*Cac* phenotype)
5) Growth with erythromycin (only possible with the plasmid, or the Erm^R gene)
6) HaloTag fluorescence (only possible with the plasmid, or the HaloTag gene)
7) Production of isopropanol (co-culture phenotype only)

The phenotype checklist of the starting co-culture partners (*Clj*-ptaHalo and wild-type *Cac*), the expected phenotype of *Cac* cells that carry the plasmid, like the *Cac*-ptaHalo strain, and the phenotype observed in the *Cac*-P4.5 strain is shown in Table 1 for comparison. All strains were negative for isopropanol production, since that phenotype is only observed in the co-culture of *Cac* and *Clj*, and only possible when both organisms are present. As such, the *Clj*-ptaHalo cells were only positive for growth on erythromycin, and the HaloTag fluorescence, and negative for all other characteristics. The wild-type *Cac* was the opposite of *Clj*-ptaHalo strain, and was positive for the first five characteristics, but not for growth on erythromycin nor the HaloTag fluorescence. It follows that any wild-type *Cac* cells that acquired the p100ptaHalo plasmid, would have a phenotype that was a sum of both parent strains (wild-type *Cac* and *Clj*-ptaHalo strains), and would be positive for all of the chosen characteristics (except the production of isopropanol, which is a co-culture specific phenotype). The isolated *Cac*-P4.5 strain matched the expected phenotype almost exactly, except for the plasmid-specific HaloTag fluorescence phenotype (Table 1).

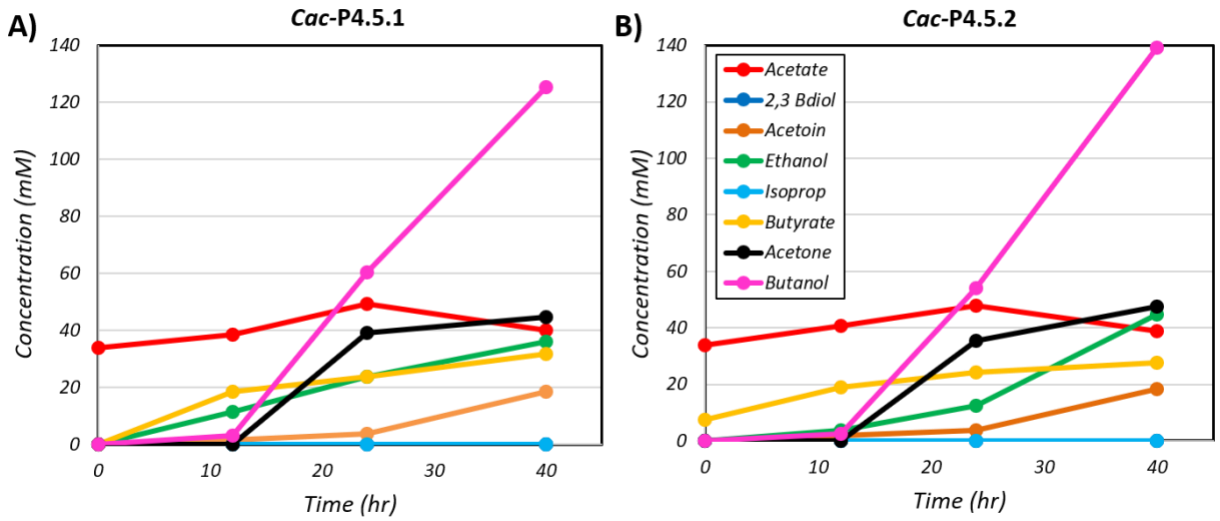

Figure 11. The metabolite profile of the *Cac*-P4.5 isolated strain. This strain showed the pure *Cac* phenotype of butanol, acetone, and acetoin production. No isopropanol was detected, indicating the selection process removed all *Clj*-ptaHalo cells. Product profiles of two biological replicates are shown.

The cells from the selection line *Cac*-P4.5 had the expected *Cac* phenotype of surviving the heat-shock, growth on glucose only, and growth on plate surface (Table 1). *Cac*-P4.5 strain also produced butanol, as well as acetone and acetoin, all of which are *Cac* specific metabolites (Figure 13). Significantly, no isopropanol nor 2,3-butanedio (co-culture specific metabolites) were detected in this strain, indicating the selection process worked at eliminating all *Clj*-ptaHalo cells

from the original co-culture (Figure 11). Per the goal of this study, the selected *Cac*-P4.5 cells also showed the evidence of acquiring the plasmid DNA from *Clj*-ptaHalo during the co-culture. The erythromycin resistance of the *Cac*-P4.5 strain can only be explained by the presence of the Erm^R gene in the selected strain, which was encoded on the p100ptaHalo plasmid (originally in the *Clj*-ptaHalo parent strain. However, the *Cac*-P4.5 strain did not show any red fluorescence when labeled with the red HaloTag ligand Janelia Fluor (Figure 12). Thus, it was not clear why the isolated strain had the Erm^R gene phenotype, but did not appear to express the HaloTag.

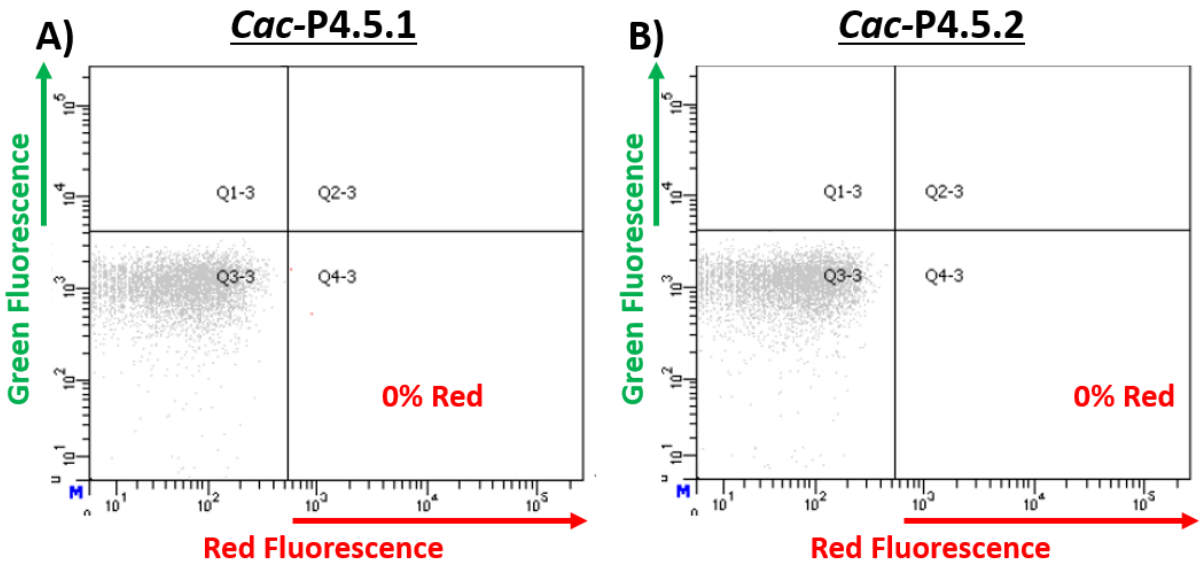

Figure 12. The results of fluorescent labeling of the *Cac*-P4.5 strain. Cells were labeled with the red Janelia Fluor®646 ligand (see Methods). No red fluorescent cells were detected using flow cytometry, indicating the lack of the HaloTag protein expression in the *Cac*-P4.5 strain. Results from two biological replicates are shown.

The *Cac*-P4.5 strain had the expected *Cac* phenotype of surviving the heat-shock, growing on glucose alone, growth on plate surface. In terms of metabolic activity, *Cac*-P4.5 cells produced butanol, as well as acetone and acetoin, all of which are *Cac*-specific metabolites (Figure 11).

Significantly, no isopropanol (the metabolite that can only be produced by the *Cac*-*Clj* co-culture) was detected in this selection line, indicating the selection process worked at eliminating all *Clj*-ptaHalo cells from the original co-culture (Figure 11). Per the goal of this study, the selected *Cac*-P4.5 cells also showed the evidence of acquiring the plasmid DNA from *Clj*-ptaHalo in the original co-culture. This is because the *Cac*-P4.5 cells were resistant to the erythromycin (Table 1). Thus, the *Cac*-P4.5 strain acquired the Erm^R gene, but could express HaloTag protein as assessed by flow cytometry analysis. This could be explained in two ways; either the HaloTag gene was lost at some point during the selection process (Figure 12), or the HaloTag gene was expressed at very low levels by the *Cac*-P4.5 strain and not detectable by flow cytometry. Therefore, at least a part of the p100ptaHalo plasmid, carrying the Erm^R gene was transferred to *Cac*. The transfer of the p100ptaHalo plasmid is examined in detail using PCR assays in the following section. To further confirm the identity of the *Cac*-P4.5 strain, its morphology was examined using transmission electron microscopy (TEM). As shown in Figure 13, after 24 hrs of growth the *Cac*-P4.5 cells had the appearance of wild-type *Cac* cells (17): they displayed large translucent regions (granulose formed in preparation for spore formation) in their cytoplasm, and a few fully formed *Cac*-P4.5 spore was observed (Figure 13A). In summary, the *Cac*-P4.5 strain showed the phenotype of wild-

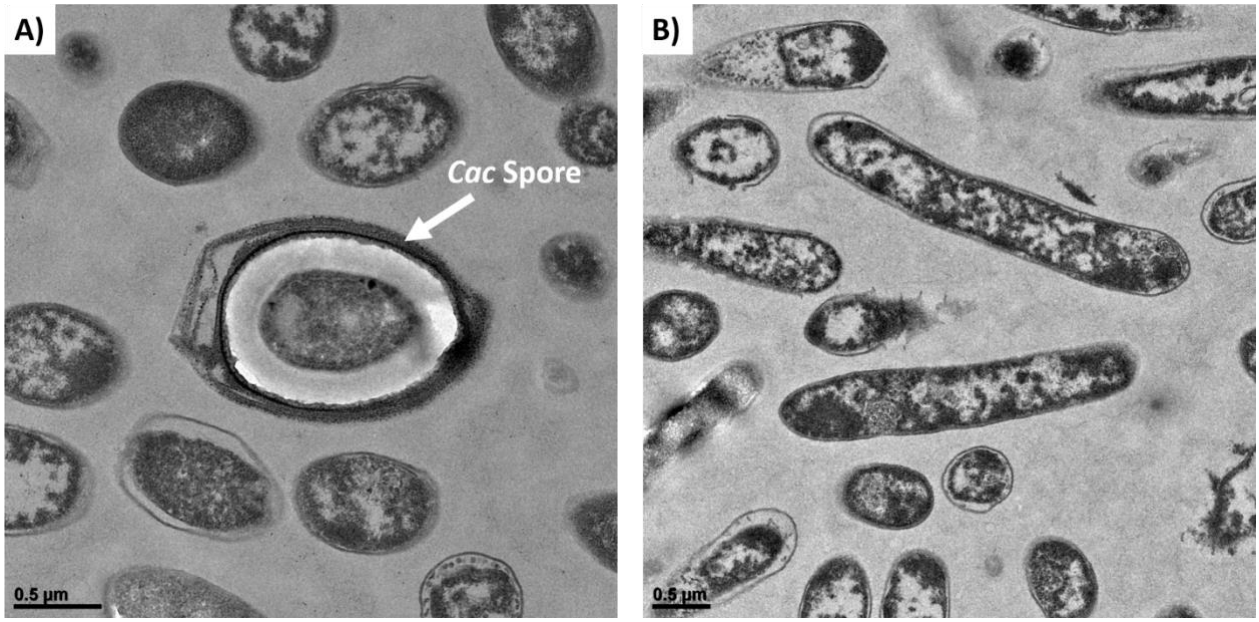

Figure 13. TEM imaging of the *Cac*-P4.5 selection cell line. A) A fully formed *Cac* spore. B) *Cac*-P4.5 cells showing the formation of granulose, which are the large white & translucent regions, consistent with the wild-type *Cac* phenotype.

type *Cac* cells (Table 1), metabolic activity of a pure wild-type *Cac* culture (Figure 11), and the cell morphology and spore formation consistent with wild-type *Cac* (Figure 13). At the same time the *Cac*-P4.5 strain was resistant to erythromycin. The latter shows that at least a part of the *Clj*-ptaHalo plasmid DNA, containing the Erm^R gene, was transferred to *Cac* from *Clj*-ptaHalo cells.

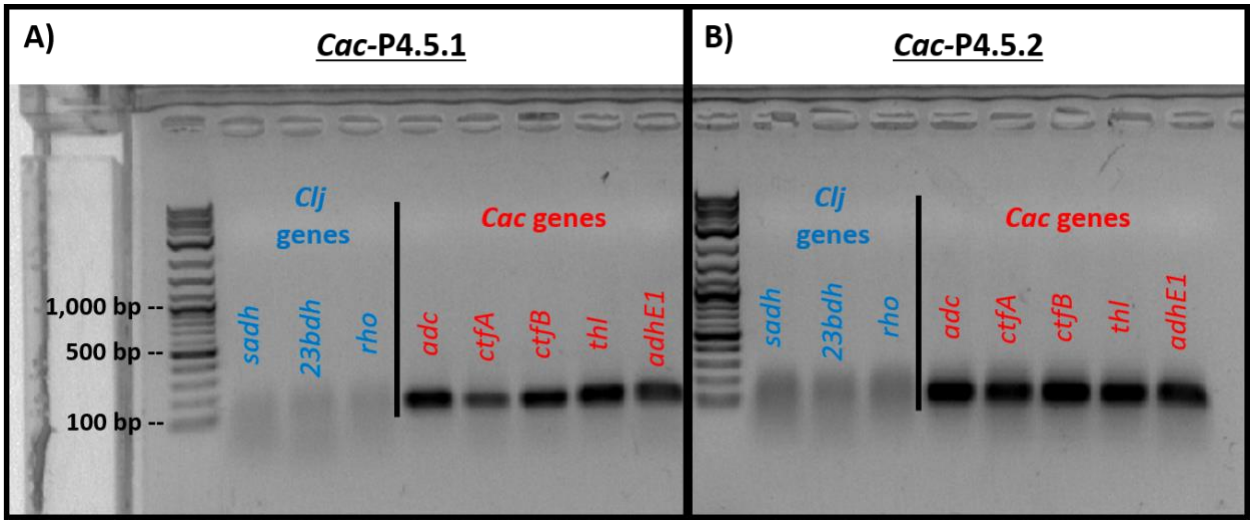

Figure 14. PCR assays used to test genomic DNA of cells from the *Cac*-P4.5 strain for three *Clj* -specific (blue) and five *Cac*-specific (red) genes. Two biological replicates are shown. In both, only the *Cac*-specific primers generated the expected ~100 bp band products. *Clj*-specific primers did not generate any product, indicating no *Clj* cells were present in the isolated strain.

X. PCR analysis of the genomic and p100ptaHalo-plasmid DNA in the Cac-P4.5 cell line. The *Cac*-P4.5 strain showed almost the exact phenotype that was expected of *Cac* that has acquired the plasmid DNA from *Clj*-ptaHalo. The only inconsistency was the lack of the HaloTag fluorescence in the *Cac*-P4.5 strain, suggesting either the lack of the HaloTag gene, or the lack of detectable HaloTag expression. To examine whether the whole or parts of the p100ptaHalo plasmid are present in the *Cac*-P4.5 strain, three PCR assays were used. First, genomic DNA of the *Cac*-P4.5 strain was tested for the presence of any *Clj*-ptaHalo genes that may be present in these cells. There was a possibility that a small number of *Clj*-ptaHalo cells was still persisting in the *Cac*-P4.5 cell line, which could break down erythromycin in the culture medium, and therefore allow *Cac*-P4.5 cells to grow. Therefore, the *Cac*-P4.5 cells were screened for 5 *Cac* genes (*adc*, *ctfA, ctfB, adhE1*, & *thl*), and 3 *Clj* genes (*sadh, 23bdh,* & *rho*). Control PCR reactions with the pure wild-type *Cac*

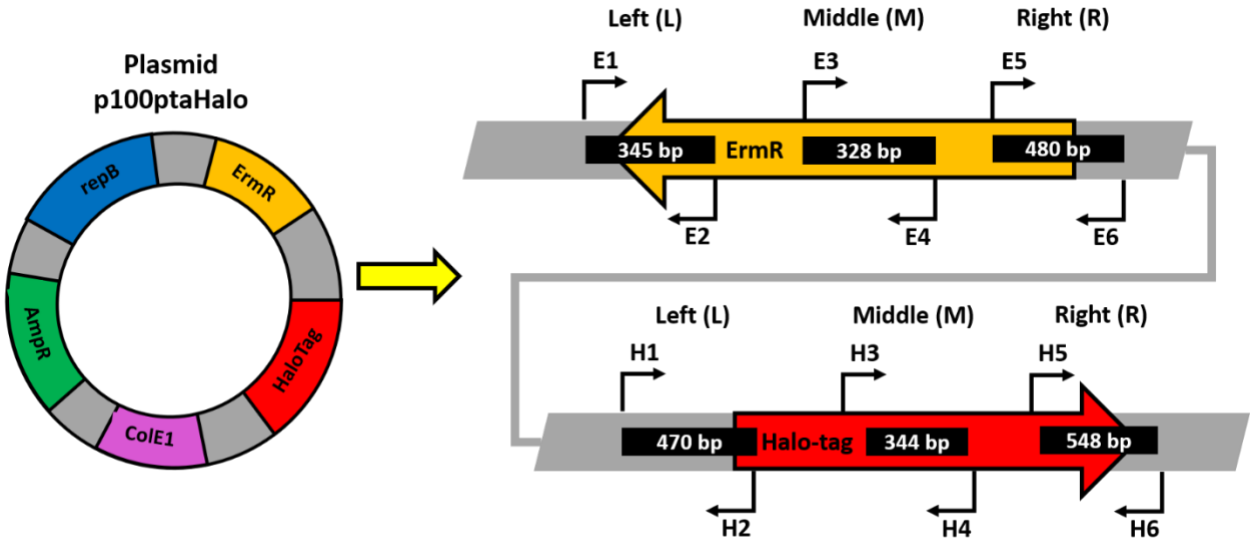

Figure 15. The overview of the p100ptaHalo plasmid. The plasmid contained the HaloTag gene (red), and the Erm^R gene (yellow). The plasmid also contained the repB ori for *Clostridium* organisms, ColE1 ori for *E. coli*, and Amp^R gene for ampicillin resistance for use in *E. coli* (see Methods). Three primer pairs were designed for each gene, as shown, to test for the left (L), middle (M), and the right (R) portions of the two target genes. Primers E1 and H1 bind outside of each gene to the left, while primers E6 and H6 bind outside of each gene to the right, to test whether the original plasmid backbone was still present in the tested selected cells.

genomic DNA produced bands (~100 bp) only with the *Cac*-specific primers. Similarly, control reactions with the pure *Clj* genomic DNA produced bands (~100 bp) only with the *Clj*-specific primers. Thus, the primers designed for the assay showed very high specificity for their target organisms. Genomic DNA from *Cac*-P4.5 strain was tested using the same PCR assays (Figure 14). Both biological replicates showed the presence of only the *Cac* genes in the samples, while *Clj* genes were not detected (Figure 14). Therefore, *Cac*-P4.5 strain must have acquired the Erm^R gene from the *Clj*-ptaHalo strain during the selection process. Of note, these results are another piece of evidence that shows the selection process used in this study (Figure 10) worked as expected i.e., over the course of the selection, it eliminated all *Clj*-ptaHalo cells, and enriched the culture in *Cac* cells that acquired p100ptaHalo-plasmid.

Genomic DNA extracts from the *Cac*-P4.5 strain were tested for the Erm^R gene, and the HaloTag gene using PCR assays. Genomic DNA samples were tested, since the genomic DNA extraction would also contain any plasmid DNA present in these cells. Control PCR reactions for both genes showed identical results for both genomic and plasmid DNA extracts from the positive control *Cac*-ptaHalo strain. Three sets of primers were designed for both genes to test either the left flank (L), the middle (M), or the right flank (R) of both genes (Figure 15). The flanking PCR reactions had one primer bind either end of the target gene, while the second primer would bind outside of the gene on the plasmid backbone (Figure 15). Genomic DNA from four biological replicates of the *Cac*-P4.5 strain was tested for the presence of the Erm^R gene, since *Cac*-P4.5 cells were resistant to erythromycin. Here, the middle (M) and right (R) PCR tests for the Erm^R gene generated the expected bands (Figure 16B). Surprisingly, the left (L) reaction did not generate the expected band in all tested colonies (Figure 16B). Since the *Cac*-P4.5 strain was resistant to erythromycin, the Erm^R gene sequence must be complete, and the primer E2 was unlikely to be the reason behind the negative PCR outcome. Thus, the reaction did not work most likely because the target sequence of the primer E1, which would bind to the left and outside of the Erm^R gene

must be missing (Figure 16). This implies that at least a portion of the p100ptaHalo plasmid, which contains the Erm^R gene, was integrated into the *Cac*-P4.5's genome. This is further supported by the lower intensity of the M & R bands produced from *Cac*-P4.5's DNA, compared to bands generated from the *Cac*-ptaHalo's DNA (positive control; Figure 16A). In both cases, the same amount of DNA template was used for the PCR reaction. *Cac*-ptaHalo cells contain multiple copies of the plasmid, and thus multiple copies of the Erm^R gene, which resulted in the strong PCR bands. If a portion of the p100ptaHalo plasmid integrated into *Cac*-P4.5's genome, each cell of that strain would only carry a single copy of the Erm^R gene, resulting in less PCR product, and thus bands with lower intensity.

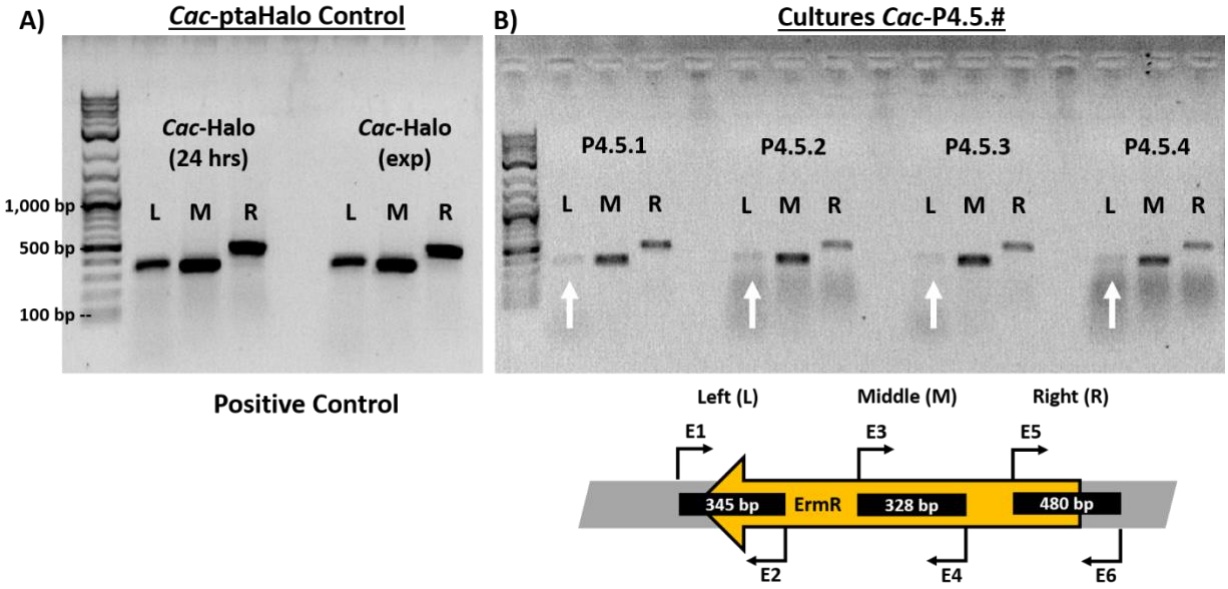

Figure 16. PCR assays used to detect the presence of the Erm^R gene in the *Cac*-P4.5 strain. A) The DNA sample from the *Cac*-ptaHalo (containing the p100ptaHalo plasmid, positive control) produced the expected bands, with strong intensity for the left (L), middle (M), and right (R) PCR reactions. B) Results of the PCR reactions on the DNA extracts from four biological replicates of the *Cac*-P4.5. In all replicates the left (L) reaction did not generate the expected band (white arrows). The middle (M) and right (R) reactions worked as expected. The M and R bands in all four samples had a lower intensity compared to the positive control. The same amount of the DNA template was used in all reactions.

The same *Cac*-P4.5 DNA samples were tested for the presence of the HaloTag gene as well. All three PCR reactions (L, M, R) of the HaloTag gene assay produced the expected bands in all four DNA samples from the *Cac*-P4.5 strain (Figure 17B). Why were the *Cac*-P4.5 cells non-fluorescent when labeled with the HaloTag ligand if they did carry the HaloTag gene? The bands generated from the *Cac*-P4.5's DNA had a lower intensity, compared again to the positive-control *Cac*-ptaHalo DNA sample (Figure 17A), similarly to the results of the Erm^R-gene assay (Figure 16). Since the same amount of DNA template was used in all PCR reactions, this again implies that the *Cac*-P4.5 strain contains fewer HaloTag gene copies, compared to the *Cac*-ptaHalo strain which carries multiple copies of the p100ptaHalo plasmid. This is further evidence for plasmid DNA integration into the *Cac*-P4.5 strain's genome. A single copy of the HaloTag gene, depending on where and how the integration event occurred, would most likely not be able to produce enough of the HaloTag protein, per each *Cac*-P4.5 cell, to reach the detection threshold of flow cytometry.

In summary, p100ptaHalo-plasmid DNA originating from the *Clj*-ptaHalo strain successfully transferred into the WT *Cac* cells during the co-culture. Over the course of the selection process (Figure 10), a portion of the plasmid containing the Erm^R and HaloTag genes integrated into *Cac*'s genomic DNA, creating the *Cac*-P4.5 strain. The integration of the portion of the p100ptaHalo plasmid fully explains the observed phenotype of the *Cac*-P4.5 strain.

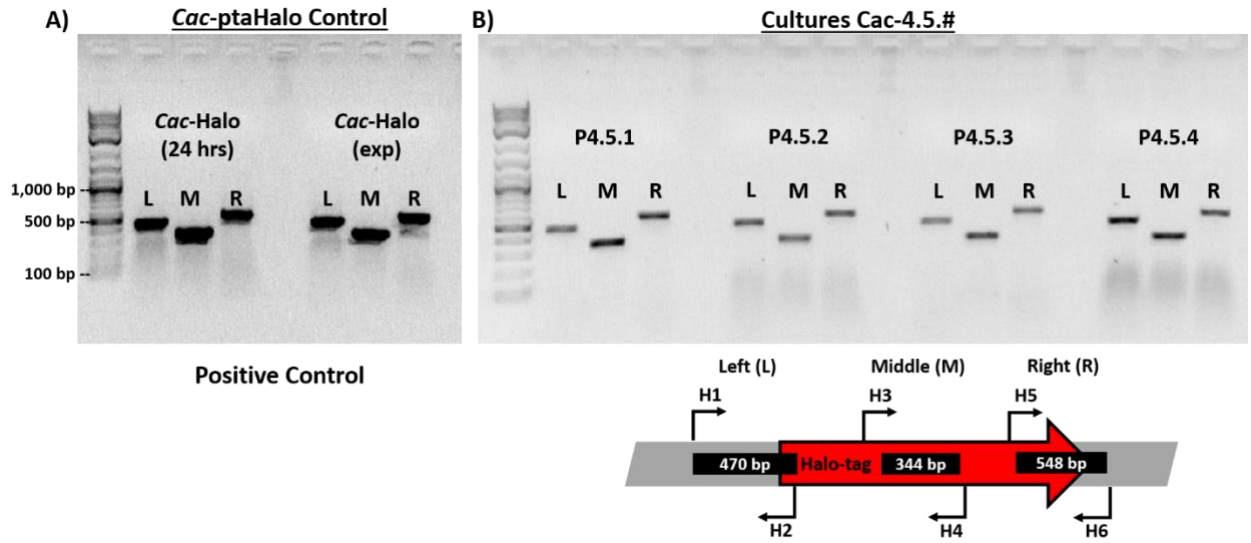

Figure 17. PCR assays used to detect the presence of the HaloTag gene in the *Cac*-P4.5 strain. A) The DNA sample from the *Cac*-ptaHalo (positive control) produced the expected bands, with strong intensity for the left (L), middle (M), and right (R) reactions. B) Results of the PCR reactions on the DNA extracts from four biological replicates of the *Cac*-P4.5 strain. All three reactions produced the expected product, implying the entire gene is present. The bands in all four samples had a lower intensity compared to the positive control. The same amount of the DNA template was used in all reactions.

XI. *C. ljungdahlii* seeks out CO_2 in novel anaerobic chemotaxis swim assay. Gas chemotaxis has been well established for physiologic gases like O_2 and nitric oxide (NO) (21), however CO_2 sensing mechanisms are less established. CO_2 sensing is thought to be widespread across plants, fungi, insects and animals, but more studies are need to pinpoint the mechanisms of Co2 sensing in bacterial systems (21). Many bacterial pathogens are thought to have developed sensing CO_2 mechanisms used to locate the perfect host environment. For example, *Bordatella (22), Bacillus (23), Borrelia (24), Vibrio (25), and Pseudomonas spp (26).* have been shown to have increased virulence gene expression, including adherence to cells and toxin production, when the CO_2 level is consistent with a mammalian host. Currently, one of the most promising candidates for CO_2 sensing mechanisms across all species is carbonic anhydrase (CA). Carbonic anhydrase is a metalloenzyme that reversibly hydrates carbon dioxide ($CO_2 + H_2O \leftrightarrow HCO_3^- + H+$) (27). There are 5 classes of carbonic anhydrases (α, β, γ, δ and ζ) (21), with α, β, and γ CA being the classes in bacterial systems (28). However, it is not clear whether CA itself does the sensing or if the conversion of CO_2 to bicarbonate transduces a change in CO_2 levels that can be used by actual CO_2 sensors in the cell (21).

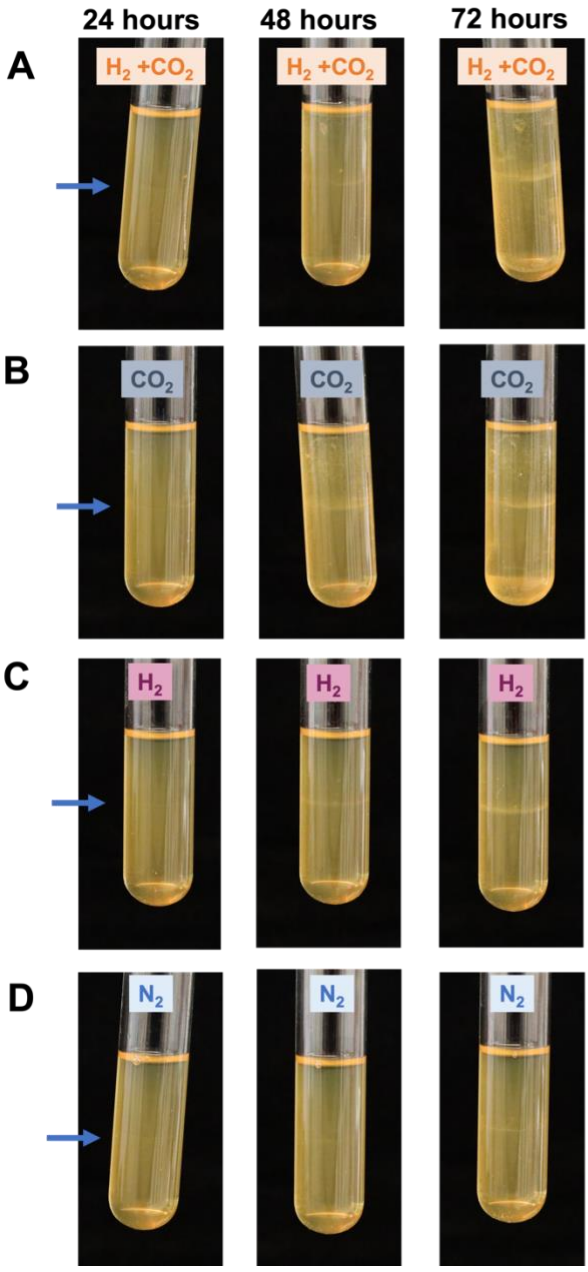

Figure 18: Novel anaerobic swim assays show movement of WT *C. ljungdahlii* towards various headspace gas mixes using RCM medium with 0.3% agar in sealed serum tubes. Arrow indicates inoculation line. A) WT *C. ljungdahlii* swims toward a 80% H_2 20% CO_2 headspace at 24, 48, and 72 hours. B) WT *C. ljungdahlii* swims toward a 100% CO_2 headspace at 24, 48, and 72 hours. C) WT *C. ljungdahlii* appears not to swim towards a 100% H_2 headspace at 24, 48, and 72 hours. D) WT *C. ljungdahlii* appears not to swim towards a 100% N_2 headspace at 24, 48, and 72 hours. Blue arrows indicate inoculation layer in agar.

To investigate how *C. ljungdahlii* and *C. acetobutylicum* are attracted to each other in co-culture, we decided to probe the ability for *C. ljungdahlii* to sense waste gases produced by *C. acetobutylicum*. A novel anaerobic swim assay was developed in sealed serum tubes in order to test the movement of *C. ljungdahlii* towards gases in the headspace. Figure 9 shows the movement of WT *C. ljungdahlii* towards 80% H_2 20% CO_2 (Fig 18A), 100% CO_2 (Fig 18B), 100% H_2 (Fig 18C), and 100% N_2 (Fig 18D) at 24, 48, and 72 hours. While both 80% H_2 20% CO_2 and 100% CO_2 show movement toward the headspace, the most prominent movement appears to be towards pure CO_2. Pure H_2 and N_2 headspace showed little to no movement of *C. ljungdahlii* away from the initial inoculation site, indicating in these particular conditions *C. ljungdahlii* was not actively seeking only H_2 or the N_2 control. To further quantitate the movement *C. ljungdahlii* toward gases, we established a qPCR based assay to count the number of genome copies (9, 29).

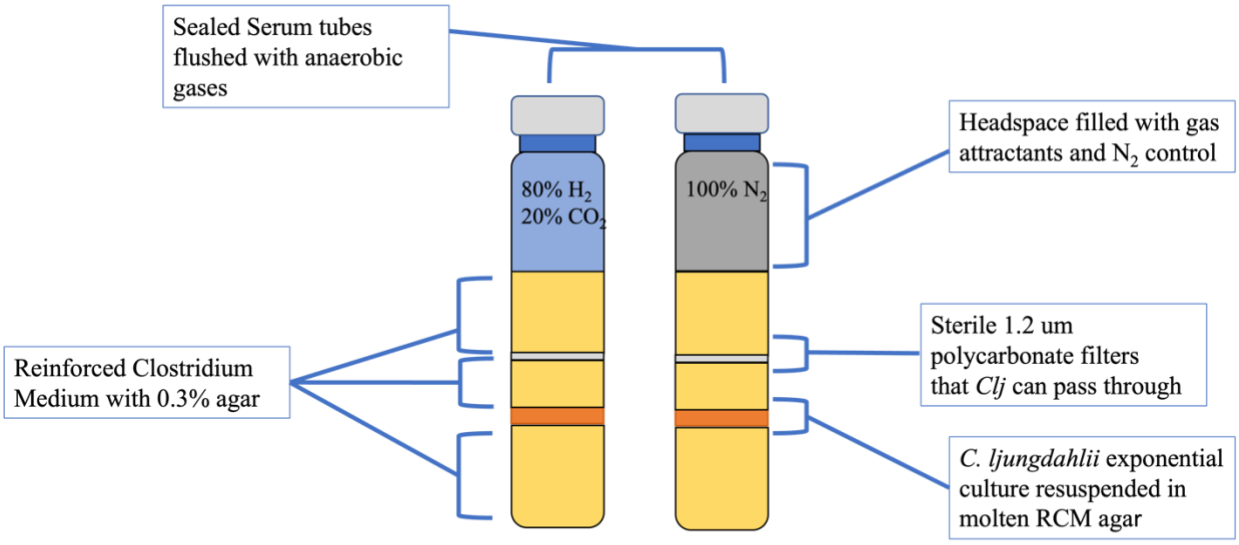

Figure 19 Schematic of chemotaxis swim tubes for quantification of *C. ljungdahlii* movement towards gases. 4 ml of reinforced clostridium medium (RCM) with 0.3% agar were added to sterile serum tubes and allowed to solidify. A layer of exponentially growing WT *C. ljungdahlii was* mixed with RCM 0.3% agar and allowed to solidify. 2 mL of RCM 0.3% agar were added and solidified. A sterile 1.2 um polycarbonate filter was placed on top of the solid agar and 4 mL of RCM 0.3% agar was used to cover the filter. Once all agar was solid tubes were sealed and flushed with either 80% H_2 20% CO_2 or 100% N_2.

New swim tubes were designed using a sterile porous (1.2 um) polycarbonate membrane embedded in the reinforced clostridium medium (RCM) swim agar **(**0.3%). Figure 19 shows a schematic of how these tubes were set up. The agar layer above the polycarbonate filter was harvested for genomic DNA extraction every 24 hours for each condition. Figure 11 shows WT *C. ljungdahlii* movement through 1.2 um pores with 80% H_2 20% CO_2 (Fig 20A), and 100% N_2 (Fig 20B) over 48 hours. Cells have clearly moved between the pores in the sterile filter to move towards the 80% H_2 20% CO_2 headspace after 48 hours. After extracting the genomic DNA from the swim agar a standard curve was performed on *C. ljungdahlii* gDNA(Fig 20C), and the qPCR method we have previously used to quantify genome copies was calculated and showed the highest genome copy number after 48 hours above the filter (Fig 20D).

XII. A potential mechanism for chemotaxis towards CO_2 in *C. ljungdahlii*. To begin the search for a potential CO_2 sensing system in *C. ljungdahlii*, we first took a look at carbonic anhydrase homologs in *Clostridium spp*. Recently, a novel β CA has been characterized in *C. autoethanogenum*, a close relative to *C. ljungdahlii*. When purified, this β CA was shown to have carbonic anhydrase activity, and functional knockout complementation in *E. coli* carbonic anhydrase knockout (30). This β CA was also shown to form as a dimer and is predicted to have a molecular weight of 14.2 kDa. *C. ljungdahlii* also has this carbonic anhydrase (CLJU_c10130), which on the WT *C. ljungdahlii* genome, is located near a putative methyl-accepting chemotaxis receptor (CLJU_c10160) and flagellar assembly machinery genes (CLJU_c10190-CLJU_c10450) (Figure 21A). Based on this location, we believe this methyl-accepting chemotaxis protein has potential to be a novel CO_2 sensor in *C. ljungdahlii*. Methyl-accepting chemotaxis proteins are the main chemotactic sensing proteins in bacteria, which include a ligand binding domain, transmembrane helices and a cytoplasmic signaling domain that interacts with downstream regulatory proteins involved in chemotaxis pathways (31) (Figure 21B). CLJU_c10160 contains regions typical to methyl-accepting chemotaxis protein signaling domains (HAMP and SD) based on homology, however the ligand binding domain does not appear to be similar to any previously characterized methyl-accepting chemotaxis protein. Many types of membrane topology exist for different known chemotaxis receptors (31), so further bioinformatic analysis is needed to elucidate the function of this particular methyl-accepting chemotaxis protein.

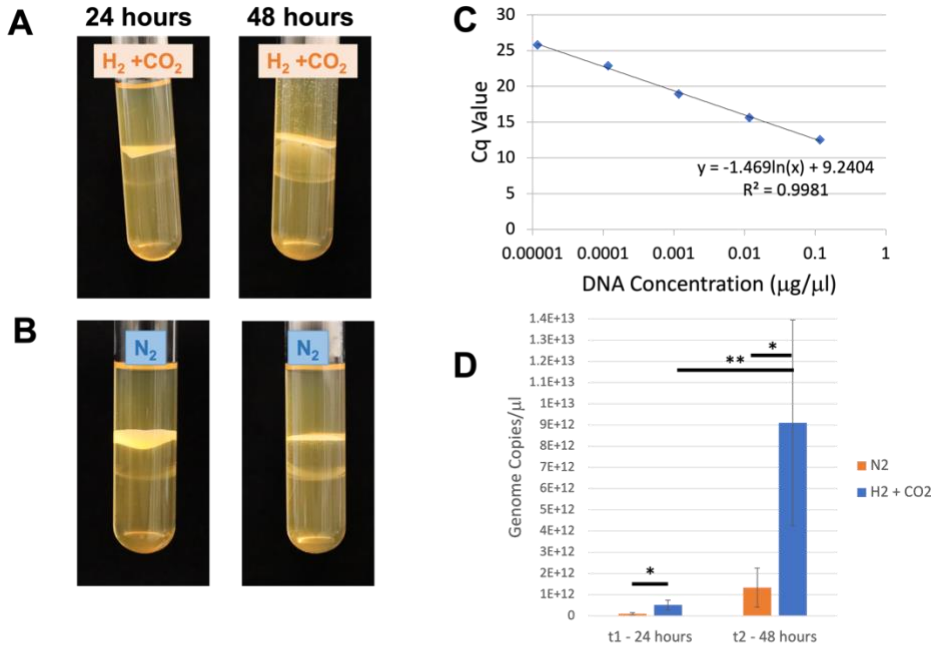

Figure 20: Quantification of cell movement towards headspace gases. Swim tubes were inoculated with exponentially growing *C. ljungdahlii* in a layer of 0.3% RCM swim agar. A 1.2 um polycarbonate membrane filter was positioned on top of fresh medium above the inoculation. A final layer of 0.3% agar was added on top of the filter. A) WT *C. ljungdahlii* movement towards 80% H_2 20% CO_2 over 48 hours. B) WT *C. ljungdahlii shows no* movement towards N_2 Headspace after 48 hours. C) Standard curve to determine DNA concentration of samples based on Cq value. This DNA concentration is then used to calculate the number of genome copies per µL. D) WT *C. ljungdahlii* genome copies per uL that passed through the sterile filter after 48 hours. Error bars represent SE, Student's t-test. n=6 except t2 $H_2 + CO_2$ (n=4) *p < 0.05, **p< 0.01.

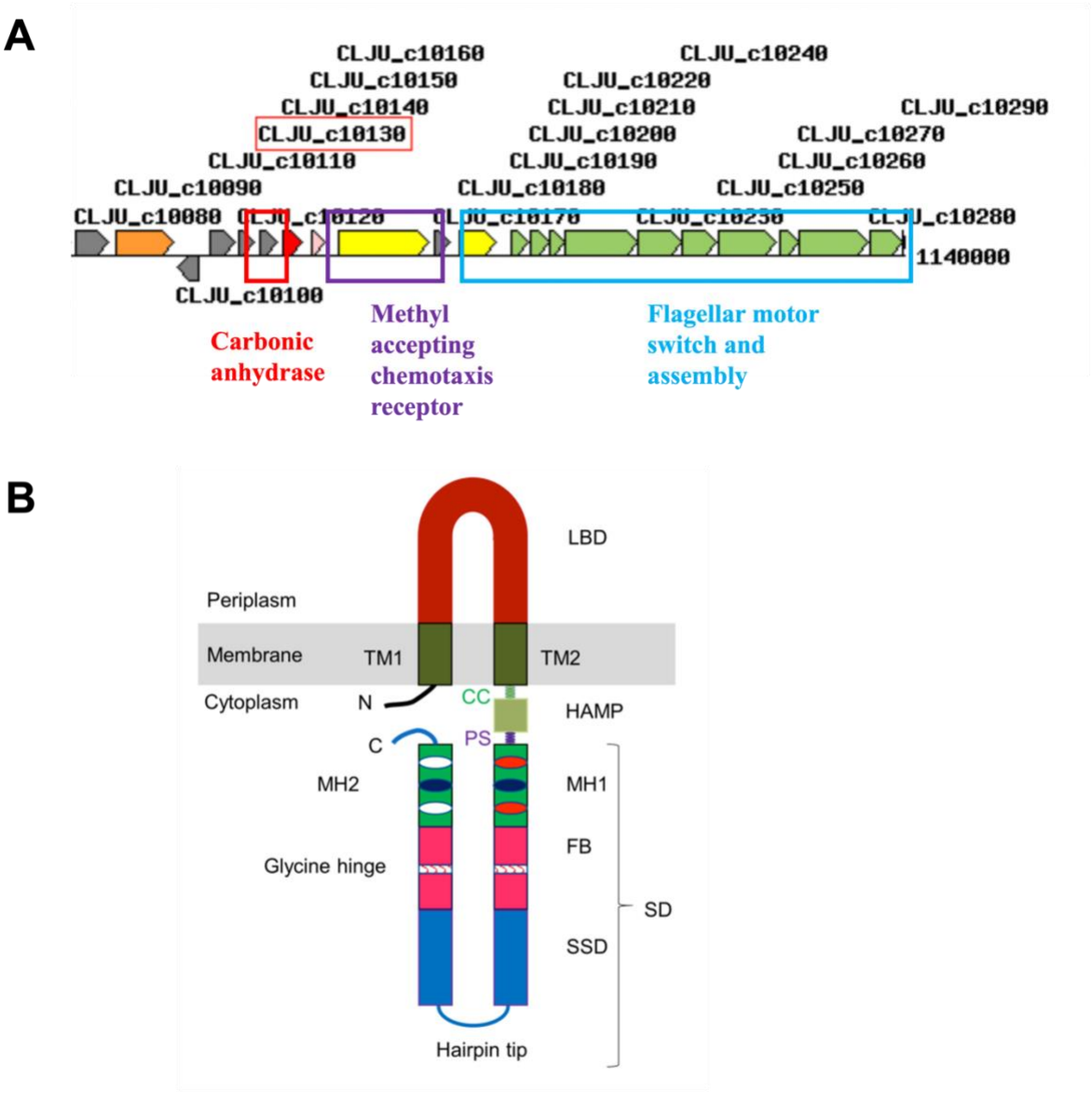

Figure 21: A potential mechanism for chemotaxis towards CO_2 in *C. ljungdahlii*. A) locus of C. ljungdahlii CA, MeChe and flagellar assembly genes in C. ljungdahlii genome (KEGG). B) Typical structure of methyl-accepting chemotaxis receptors in bacteria. LBD ligand binding domain, TM transmembrane helix, CC control cable, HAMP histidine kinase, adenyl cyclase, methyl-accepting chemotaxis protein and phosphatase region, PS phase stutter, SD signaling domain, MH methylation helix, FB flexible bundle, SSD signaling subdomain. (from A. I. M. Salah Ud-Din, A. Roujeinikova 2017)

XIII. Putative methyl-accepting chemotaxis receptor and carbonic anhydrase show significant increase in fold change under low CO_2 concentrations in *C. ljungdahlii*. To test if CLJU_c10160 is upregulated in conditions where *C. ljungdahlii* needs gases to survive, we compared the fold change of expression for both CA (CLJU_c10130) and MeChe (CLJU_c10160) grown on only 80% H_2 20% CO_2 to N_2 and 5g/L fructose. Interestingly, MeChe had a fold change of 194.8 ± 90.4, while CA

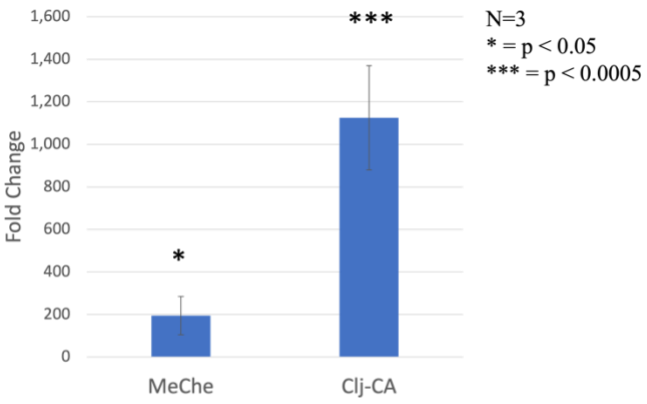

Figure 22: Fold change of methyl-accepting chemotaxis receptor (CLJU_c10160) and carbonic anhydrase (CLJU_c10130) grown on 80% H_2 20% CO_2 compared to N_2 and fructose after 6 hours. N=3 * = p < 0.05, *** = p < 0.0005 Student's t-test.

has a fold change 1,124.4 ± 245.1 when comparing growth on only gases and growth on only fructose (Figure 22). This is consistent with other bacterial carbonic anhydrases in low CO_2 conditions (32). This leads us to believe that these proteins may be involved in the mechanism that *C. ljungdahlii* uses to sense CO_2 in the environment. To further investigate the role of this methyl-accepting chemotaxis protein, we plan to knock out MeChe from the *C. ljungdahlii* genome and determine if this protein is necessary for sensing CO_2 in the environment as well as for sensing *C. acetobutylicum* in co-culture.

XIV. A fluorescent fusion protein of *Clj*-MCP and *Clj*-CA using HaloTag.

To further study *Clj*-CA and *Clj*-MCP, a fluorescent fusion protein was created with HaloTag and a flexible protein linker that was previously used for creating a fluorescent fusion with FAST (2). First, a Gblock containing the pta promoter, optimized *Clj* RBS, BamHI restriction site and HaloTag with the flexible linker (ggaggtggaggaagc) was designed and cloned into a p100_MCS based vector. This plasmid can then be cut with BamHI and any genome-amplified gene can be inserted into the cut site to create a HaloTag fluorescent fusion tag on the C-terminus of a protein of interest. Here we added *Clj*-MCP and *Clj*-CA to the p100ptalinker plasmid to create p100ptaMCP-Halo and p100CA-Halo (Figure 23).

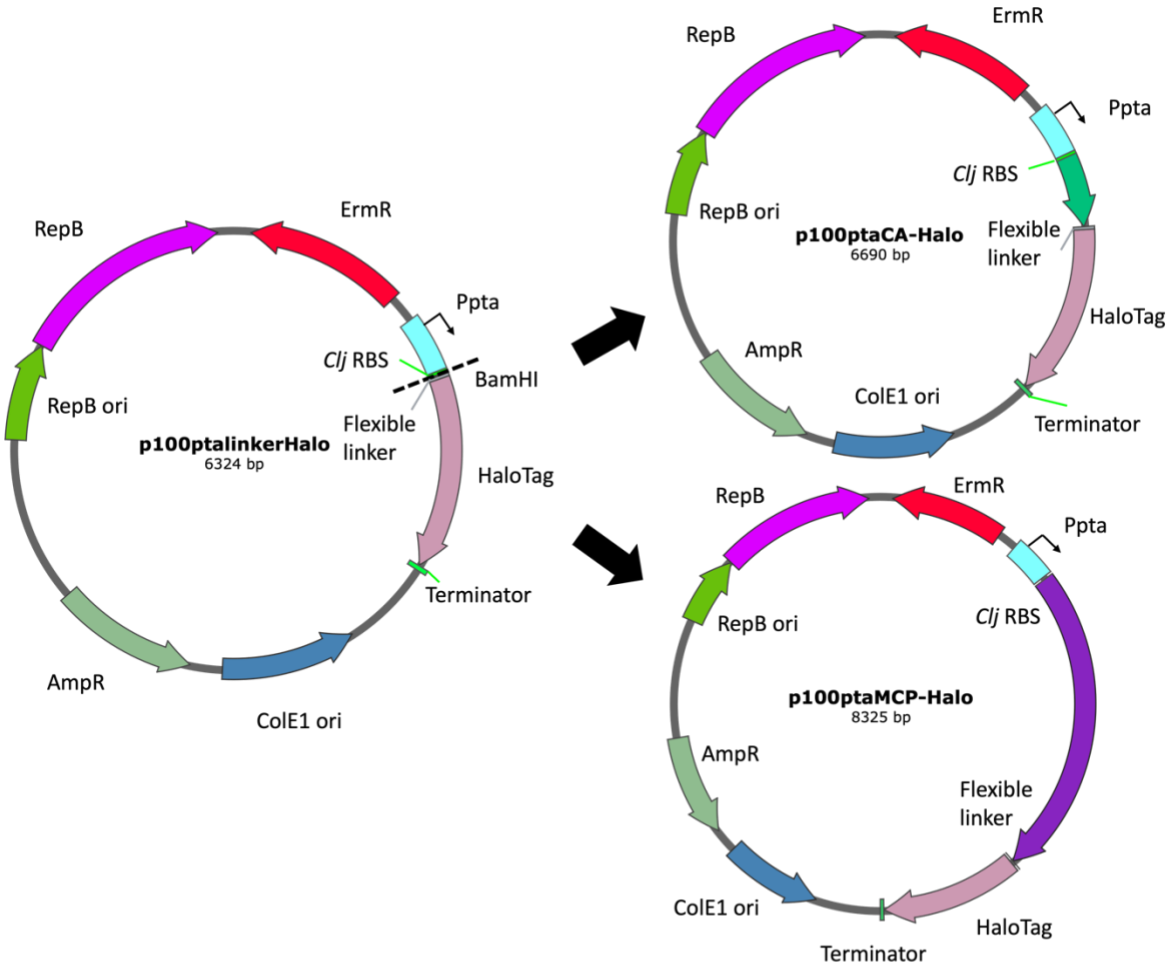

Figure 23: Vector design for p100ptalinkerHalo (left), p100ptaCA-Halo (top right), p100ptaMCP-Halo (bottom right). Ppta: promoter for C. ljungdahlii phosphotransacetylase gene (*pta*), *Clj* RBS: *C. ljungdahlii* optimized ribosome binding site (Ueki et al 2014), BamHI: BamHI restriction enzyme cut site, HaloTag: codon optimized HaloTag for *Clostridium,* Terminator: *Clostridium* rho independent terminator (*C. acetobutylicum adc* gene). ColE1 ori: Gram-negative origin of replication, AmpR: ampicillin resistance gene, RepB ori: Gram-positive origin of replication, RepB: protein that initiates replication, ErmR: Erythromycin resistance gene, *Clj*-CA: *C. ljungdahlii* carbonic anhydrase (CLJU_c10130), *Clj*- MCP: *C. ljungdahlii* Methyl-accepting chemotaxis receptor (CLJU_c10160). Vector maps generated with SnapGene.

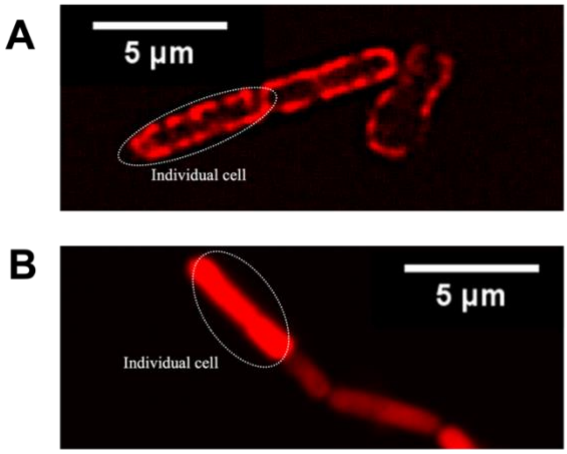

Figure 24: Fluorescent fusion proteins of *Clj*-MCP (A) and *Clj*-CA (B) using codon optimized HaloTag and a flexible linker. Circled areas indicate individual cells.

When expressed in *C. ljungdahlii*, *Clj*-MCP-Halo shows fluorescence around the outer edge of the cells near the cell membrane (Figure 24A). This suggests that *Clj*-MCP is a transmembrane or membrane anchored MCP. *Clj*-CA-Halo, however, does not appear to localize in any particular area of the cell and remains in the cytosol (Figure 24B). This is consistent with previous evidence of other CA localization within the cytosol (33).

XV. A fluorescent co-culture including *C. ljungdahlii* CA-Halo and MCP-Halo.

C. acetobutylicum and *C. ljungdahlii* have shown evidence of exchange of metabolites (9), and also protein and RNA (34). To test whether *C. ljungdahlii* CA-Halo and MCP-Halo have an impact on the previous observation of fluorescent cellular material exchange, a co-culture of *C. acetobutylicum* ZapA-FAST (2) and *C. ljungdahlii* ptaHalo (35) were compared to *C. acetobutylicum* ZapA-FAST paired with either *C. ljungdahlii* CA-Halo or *C. ljungdahlii* MCP-Halo. In the *C. acetobutylicum* ZapA-FAST and *C. ljungdahlii* ptaHalo co-culture, a small number of cells (0.78%) show both red and green fluorescence after 4 hours, but double positive cells increase to 3.68% after 9 hours in co-culture (Figure 4.7A). When *C. acetobutylicum* ZapA-FAST is paired with *C. ljungdahlii* CA-Halo, after 4 hours a similarly small number of cells (0.99%) show both red and green fluorescence after 4 hours, with less double positive cells (1.39%) compared to *C. ljungdahlii* ptaHalo after 9 hours (Figure 4.7B). Similarly, *C. acetobutylicum* ZapA-FAST paired with *C. ljungdahlii* MCP-Halo showed few cells (0.55%) with red and green fluorescence after 4 hours and lower double positive cells (1.82%) after 9 hours compared to *C. ljungdahlii* ptaHalo.

When cells from *C. acetobutylicum* ZapA-FAST and *C. ljungdahlii* CA-Halo co-culture are observed with microscopy, evidence of cells containing both green ZapA-FAST and red CA-Halo are observed. Cells with both green ZapA-FAST localization (bottom cell) and red CA-Halo (top and bottom cell) were observed in co-culture (Figure 4.8A). The localization pattern of ZapA-FAST on the bottom cell is indicative of a *C. acetobutylicum* cell with ZapA-FAST (2) localizing to the poles of the cell. CA-Halo appears to be distributed throughout the cytosol, as seen in Figure 4.6B, of both cells. It is possible that the top cell is a *C. ljungdahlii* cell and the bottom cell is a *C. acetobutylicum* cell, and ZapA-FAST and CA-Halo are being exchanged between the two. In another cell, ZapA-FAST appears to localize to only one of the cell poles, which is consistent with the localization pattern of ZapA-FAST expressed in *C. ljungdahlii* (35). This cell also contains CA-Halo, leading us to believe that this is a *C. ljungdahlii cell* that may

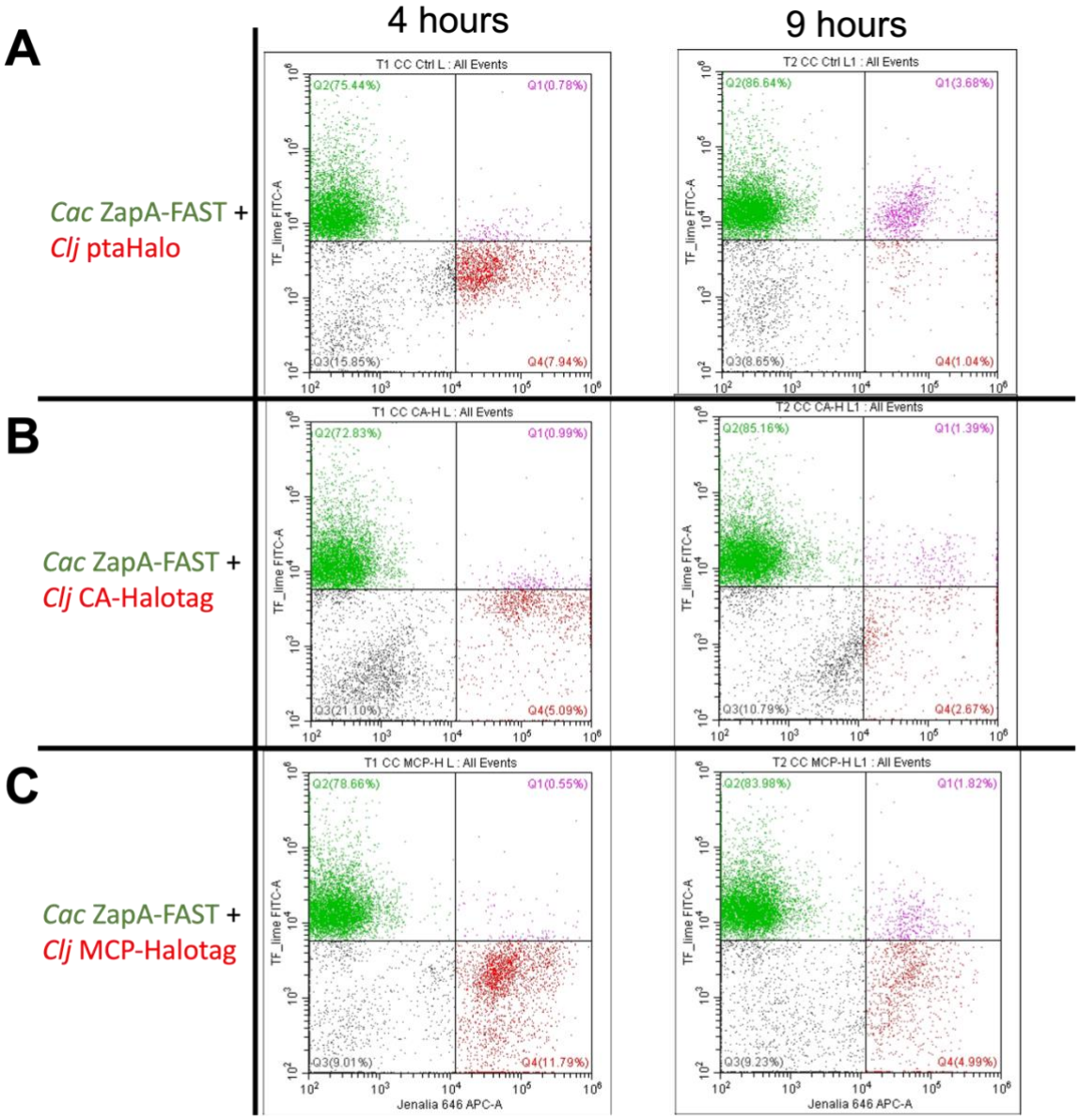

Figure 25: Flow cytometry co-culture of *C. acetobutylicum* ZapA-FAST (green) and *C. ljungdahlii* fluorescent fusion proteins (red). Purple cells indicate cells that contain both green and red fluorescent signals. A) Co-culture of *C. acetobutylicum* ZapA-FAST (green) and *C. ljungdahlii* ptaHalo (red) after 4 hours (left) and 9 hours. B) Co-culture of *C. acetobutylicum* ZapA-FAST (green) and *C. ljungdahlii* CA-Halo (red) after 4 hours (left) and 9 hours. C) Co-culture of *C. acetobutylicum* ZapA-FAST (green) and *C. ljungdahlii* MCP-Halo (red) after 4 hours (left) and 9 hours. Grey cells indicate cells that are do not contain green or red signal.

have taken up ZapA-FAST from *C. acetobutylicum* (Figure 4.8B). Evidence of *C. acetobutylicum* uptake of CA-Halo is also shown in co-culture, with what appears to be a dividing *C. acetobutylicum* ZapA-FAST cell that has ZapA-FAST localization at both the poles and the center of the dividing cell. This cell also appears to contain CA-Halo, showing evidence that CA-Halo can be taken up by *C. acetobutylicum* (Figure 4.8C). While these protein exchange

events happen infrequently in *C. acetobutylicum* ZapA-FAST and *C. ljungdahlii* CA-Halo co-culture, protein exchange still appears to be possible when overexpressing CA-Halo.

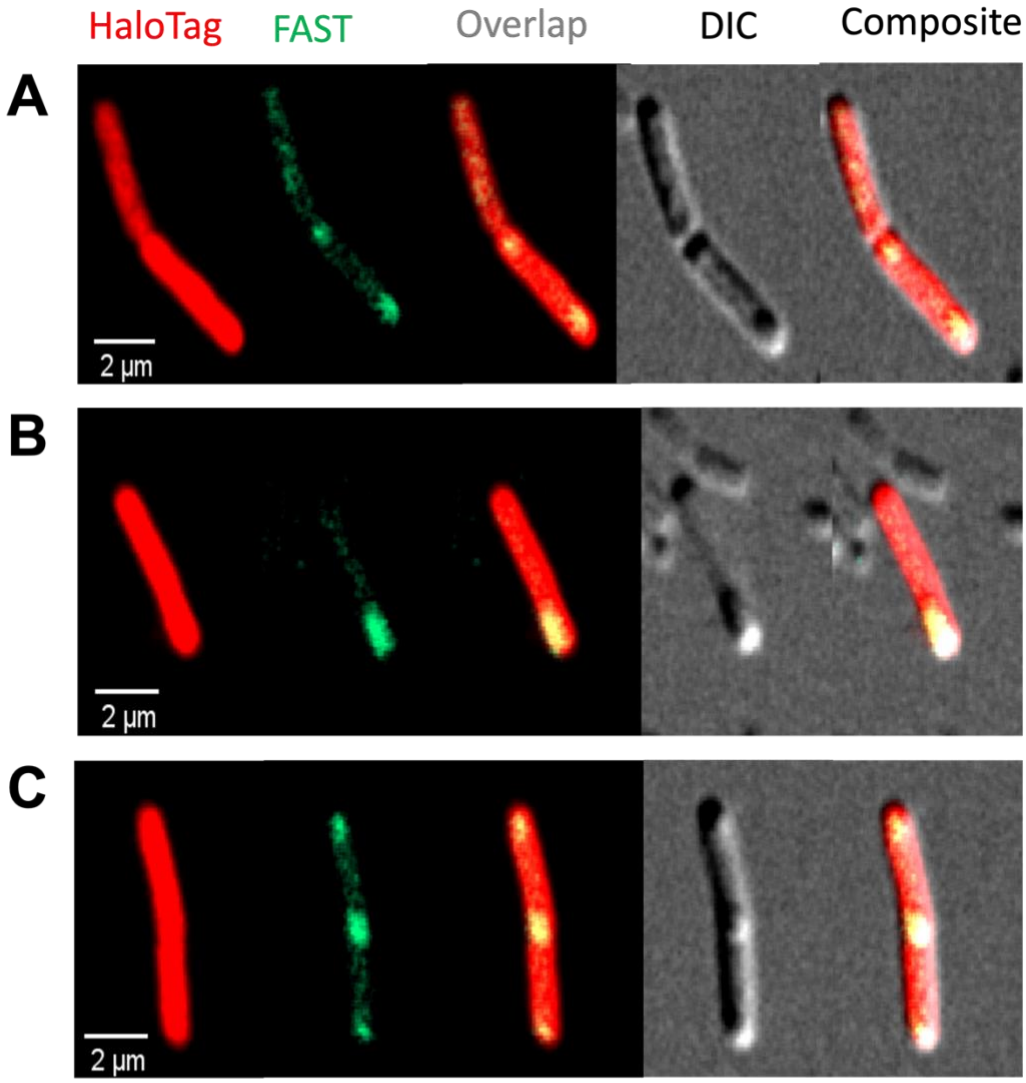

Figure 26: *C. acetobutylicum* ZapA-FAST and *C. ljungdahlii* CA-Halo co-culture cells that contain both green and red signal. A) Two cells showing exchange of both red and green fluorescent proteins. B) Cell showing *C. ljungdahlii* ZapA localization pattern and HaloTag labeling. C) Two cells showing *C. acetobutylicum* ZapA localization and HaloTag labeling.

It is unclear how *C. ljungdahlii* CA-Halo and MCP-Halo impact the exchange of fluorescent proteins in co-culture, however, overexpression of each protein of interest may impact the ability to sense attractants that are produced by *C. acetobutylicum*. For example, if *Clj*-CA is used to increase intracellular concentrations of CO_2, overexpression of *Clj*-CA may increase efficiency of retaining high intracellular CO_2 levels, reducing the need for *C. ljungdahlii* to move towards gases. *C. ljungdahlii* MCP-Halo appears to be a transmembrane or membrane

anchored MCP (Figure 24A) and overexpression of Clj-MCP may block the mechanism for exchanging intracellular materials by crowding the cell membrane.

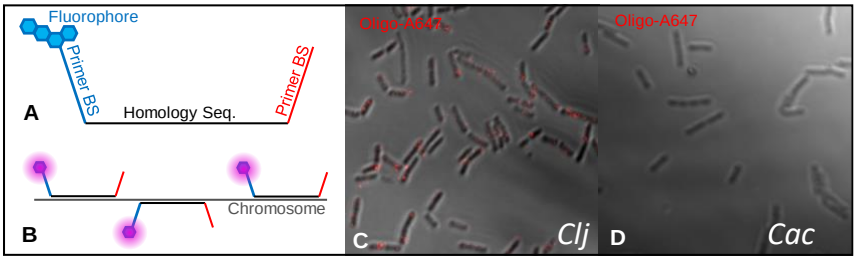

Figure 27. (A) Schematic of an oligopaint. **(B)** Schematic of chromosomal labelling via DNA-FISH. **(C)** Small fluorescent localizations appears where *Clj*'s chromosome has been labelled with the *Clj*-specific library. **(D)** The library does not label *Cac*.

XVI. Oligonucleotide based fluorescent techniques for tracking nucleic acid transfer during fusion.

Hybrid cells contain a genetic amalgam of the fusion partner's chromosomes and RNA, but the spatio-temporal dynamics of this form of nucleic acid transfer are unknown. To analyze dynamics of DNA and RNA exchange during hybridization, the development of robust and programmable visualization tools is critical. RNA-FISH is a modality of *fluorescence in situ hybridization* which targets species specific 23S ribosomal subunit sequences with complementary 18-bp oligonucleotide probes. DNA-FISH is an analogous technique which uses a library of 'oligopaints' to label the chromosome. An 'oligopaint' is a 70-86 bp oligonucleotide with three distinct regions. A central 28-44 bp region bares homology to a target chromosomal sequence and is flanked by 21 bp primer binding sites(36). Oligopaints are generated in libraries containing hundreds of unique oligonucleotides(37). Each oligopaint, while retaining the same terminal 21 bp primer binding sites, has a unique, central homology region allowing hybridization to only one position on the chromosome (Figure 27A). The homology regions are generated bioinformatically to ensure uniform binding thermodynamics, prevent secondary structure formation, and regulate the number of probe binding sites per length of chromosome(38). Then the oligonucleotides are synthesized without fluorophores through a commercial vendor. The common primer binding sites allow fluorescent molecules such as Alexa 647 or Cy5.5 to be attached to the 5' end of every 'oligopaint' *en masse* using routine procedures such as real-time PCR and *in vitro* transcription. The cells are first fixed and permeabilized (39). Then the DNA is denatured, allowing the probes to fall into an energetically favorable duplex with the chromosome. Subsequently, unbound probes are washed away.

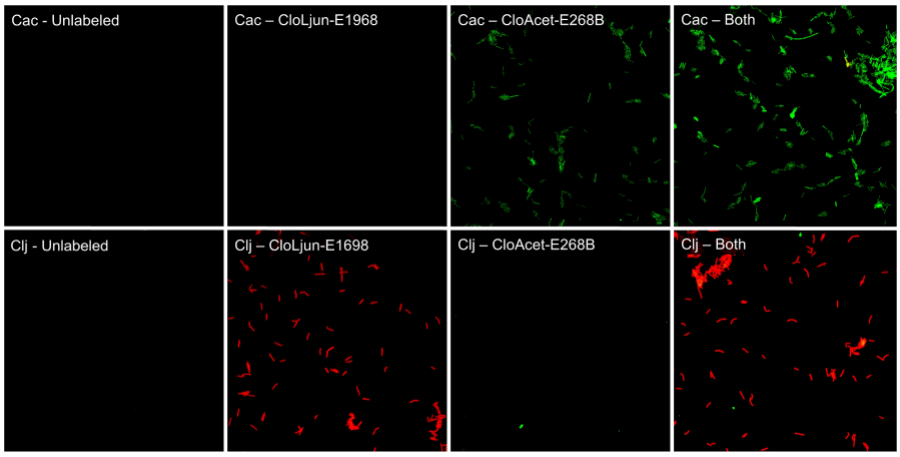

Figure 28. CloLjun-E1698 and CloAcet-E268B label orthogonally as shown by fluorescent signal only when the library is matched with its target species.

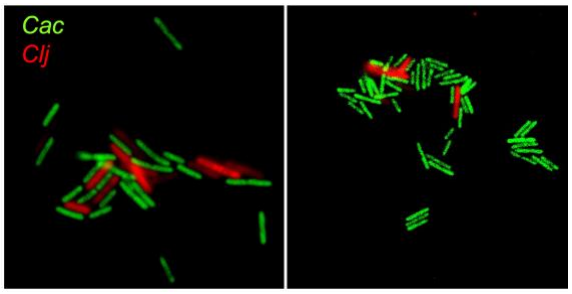

Figure 29. *Cac* and *Clj* identified via RNA-FISH in a synthetic microbial community.

The SILVA ribosomal RNA database was used in conjunction with ARB to determine species specific sequences on the 23S subunit of *Clj* and *Cac*. The probes with fluorophores were generated by a commercial vendor. The 2 probes are designated CloLjun-E1968 and CloAcet-E268B and label *Clj* and *Cac* respectively. An RNA-FISH labelling procedure for Gram-positive was adapted for use with *Cac* and *Clj*. Cultures were imaged on a Zeiss LSM880. Figure 28 shows that labelling is orthogonal, and Figure 29 shows that the probes can be used in conjunction to identify the species of *Cac* and *Clj* in synthetic co-cultures. Simultaneously, an oligopaint library specific to Clj was designed with the Oligominer web utility and synthesized with through a commercial vendor. Alexa fluor 647 was then attached to the library. The labelling procedure used for RNA-FISH was adapted for use with DNA-FISH. Pure cultures of *Clj* were labeled with the probe and imaged via confocal microscopy as can be seen in Figure 27B.

XVII. Development of a Transposon Insertion Library for investigation of genes involved in membrane fusion events.

Transposon Insertion Sequencing (TIS) is a forward genetic approach designed to assign gene essentiality and gene function (40). Transposases are enzymes which insert and excise specific genetic elements, called transposons, into and out of the chromosome. A transposon landing inside a gene's locus disrupts the gene, effectively disabling the gene function. Transposases insert transposons randomly, making the system a viable bases for random mutagenesis. Libraries of mutants created via random transposon insertion are called Transposon Insertion Libraries (TILs)(41). A major benefit to creating TILs is that each mutation is 'barcoded' with the transposon. Using Next Generation Sequencing (NGS), the unique insertion location of transposons in millions of mutants is catalogued at once(41). As insertion is random, insertion sites should be regularly dispersed throughout the genome except when the insertion is either detrimental or beneficial to the fitness of the cell. If the insertion grants a competitive advantage to the mutant, it will outcompete other mutants. Since disruption of an essential gene will be outcompeted by other mutants during growth, the TIL includes only a few essential gene disruptions, if any.

We have successfully constructed a *Clj* TIL using a Himar1C9 transposase (42) under a bi-directional anhydrotetracycline (aTc) inducible promoter which successfully constructed TIL of *C. autoethanogenum* (43) (Figure 30). The library consists of roughly $3.5x10^6$ mutants with a transposition

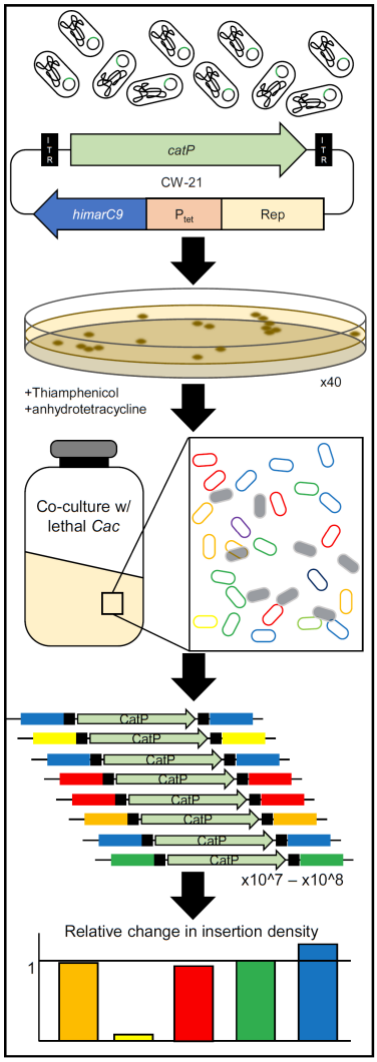

Figure 30. The TIS process. Transposition is induced from cells carrying the CW-21 plasmid. The library is collected and grown with lethal *Cac* cell to select for mutants which cannot fuse. The barcode is used to amplify the flanking regions of chromosome. NGS is used to find the relative change in insertion frequency for all possible mutants.

frequency of .029 %. False positive rate was 1.2%. False positive colonies have not undergone transposition but were able to survive selection due to plasmid retention in the presence of aTc. The TIL can be combined with synthetic biology tools to identify genes contributing to the heterogenous cell fusion.

6. Bibliography.

1. Charubin K, Bennett RK, Fast AG, Papoutsakis ET. 2018. Engineering Clostridium organisms as microbial cell-factories: challenges & opportunities. Metabolic Engineering 50:173-191.
2. Streett HE, Kalis KM, Papoutsakis ET. 2019. A Strongly Fluorescing Anaerobic Reporter and Protein-Tagging System for Clostridium Organisms Based on the Fluorescence-Activating and Absorption-Shifting Tag Protein (FAST). Applied and Environmental Microbiology 85:e00622-19.
3. Los GV, Wood K. 2007. The HaloTag: a novel technology for cell imaging and protein analysis. Methods Mol Biol 356:195-208.
4. Los GV, Encell LP, McDougall MG, Hartzell DD, Karassina N, Zimprich C, Wood MG, Learish R, Ohana RF, Urh M, Simpson D, Mendez J, Zimmerman K, Otto P, Vidugiris G, Zhu J, Darzins A, Klaubert DH, Bulleit RF, Wood KV. 2008. HaloTag: a novel protein labeling technology for cell imaging and protein analysis. ACS Chem Biol 3:373-82.
5. Popa I, Berkovich R, Alegre-Cebollada J, Badilla CL, Rivas-Pardo JA, Taniguchi Y, Kawakami M, Fernandez JM. 2013. Nanomechanics of HaloTag tethers. J Am Chem Soc 135:12762-71.
6. Jones SW, Fast AG, Carlson ED, Wiedel CA, Au J, Antoniewicz MR, Papoutsakis ET, Tracy BP. 2016. CO2 fixation by anaerobic non-photosynthetic mixotrophy for improved carbon conversion. Nat Commun 7:12800.
7. Ueki T, Nevin KP, Woodard TL, Lovley DR. 2014. Converting carbon dioxide to butyrate with an engineered strain of Clostridium ljungdahlii. MBio 5:e01636-14.
8. Mermelstein LD, Papoutsakis ET. 1993. In vivo methylation in Escherichia coli by the Bacillus subtilis phage phi 3T I methyltransferase to protect plasmids from restriction upon transformation of Clostridium acetobutylicum ATCC 824. Appl Environ Microbiol 59:1077-1081.
9. Charubin K, Papoutsakis ET. 2019. Direct cell-to-cell exchange of matter in a synthetic Clostridium syntrophy enables CO2 fixation, superior metabolite yields, and an expanded metabolic space. Metab Eng 52:9-19.
10. Wenjun Zhou, Hee Chol Kang, Mike O'Grady, Kevin M. Chambers, Brad Dubbels, Penny Melquist, Gee KR. 2016. CellTrace™ Far Red & CellTracker™ Deep Red-long term live cell tracking for flow cytometry and fluorescence microscopy. Journal of Biological Methods 3.
11. Streett HE, Kalis KM, Papoutsakis ET. 2019. A strongly fluorescing anaerobic reporter and protein-tagging system for Clostridium organisms based on the Fluorescence-Activating and Absorption-Shifting Tag (FAST) protein. doi:10.1128/AEM.00622-19.
12. Tracy BP, Gaida SM, Papoutsakis ET. 2008. Development and Application of Flow-Cytometric Techniques for Analyzing and Sorting Endospore-Forming Clostridia ▿ †, p 7497-506, Appl Environ Microbiol, vol 74.
13. Keppler A, Gendreizig S, Gronemeyer T, Pick H, Vogel H, Johnsson K. 2003. A general method for the covalent labeling of fusion proteins with small molecules in vivo. Nature Biotechnology 21:86-89.
14. Streett HE, Kalis KM, Papoutsakis ET. 2019. A strongly fluorescing anaerobic reporter and protein-tagging system for *Clostridium* organisms based on the Fluorescence-Activating and Absorption-Shifting Tag (FAST) protein. Applied and Environmental Microbiology doi:10.1128/AEM.00622-19:AEM.00622-19.
15. Demuez M, Cournac L, Guerrini O, Soucaille P, Girbal L. 2007. Complete activity profile of Clostridium acetobutylicum FeFe -hydrogenase and kinetic parameters for endogenous redox partners. Fems Microbiology Letters 275:113-121.

16. Guerrini O, Burlat B, Leger C, Guigliarelli B, Soucaille P, Girbal L. 2008. Characterization of two 2 4Fe4S ferredoxins from Clostridium acetobutylicum. Current Microbiology 56:261-267.
17. Charubin K, Modla S, Caplan JL, Papoutsakis ET. 2020. Interspecies Microbial Fusion and Large-Scale Exchange of Cytoplasmic Proteins and RNA in a Syntrophic Clostridium Coculture. mBio 11.
18. Charubin K, Streett H, Papoutsakis ET. 2020. Development of Strong Anaerobic Fluorescent Reporters for Clostridium acetobutylicum and Clostridium ljungdahlii Using HaloTag and SNAP-tag Proteins. Appl Environ Microbiol 86.
19. Johnston C, Martin B, Fichant G, Polard P, Claverys JP. 2014. Bacterial transformation: distribution, shared mechanisms and divergent control. Nature Reviews Microbiology 12:181-196.
20. Grohmann E, Muth G, Espinosa M. 2003. Conjugative plasmid transfer in gram-positive bacteria. Microbiology and Molecular Biology Reviews 67:277-+.
21. Cummins EP, Selfridge AC, Sporn PH, Sznajder JI, Taylor CT. 2014. Carbon dioxide-sensing in organisms and its implications for human disease. Cellular and Molecular Life Sciences 71:831-845.
22. Hester SE, Lui MH, Nicholson T, Nowacki D, Harvill ET. 2012. Identification of a CO2 Responsive Regulon in Bordetella. Plos One 7:12.
23. Bongiorni C, Fukushima T, Wilson AC, Chiang C, Mansilla MC, Hoch JA, Perego M. 2008. Dual promoters control expression of the Bacillus anthracis virulence factor AtxA. Journal of Bacteriology 190:6483-6492.
24. Gilmore RD, Mbow ML, Stevenson B. 2001. Analysis of Borrelia burgdorferi gene expression during life cycle phases of the tick vector Ixodes scapularis. Microbes and Infection 3:799-808.
25. Shimamura T, Watanabe S, Sasaki S. 1985. Enhancement of enterotoxin production by carbon dioxide in Vibrio cholerae. Infection and immunity 49:455-456.
26. Lotlikar SR, Hnatusko S, Dickenson NE, Choudhari SP, Picking WL, Patrauchan MA. 2013. Three functional β-carbonic anhydrases in Pseudomonas aeruginosa PAO1: role in survival in ambient air. Microbiology (Reading) 159:1748-1759.
27. Lindskog S. 1997. Structure and mechanism of carbonic anhydrase. Pharmacol Ther 74:1-20.
28. Supuran CT, Capasso C. 2017. An Overview of the Bacterial Carbonic Anhydrases. Metabolites 7:56.
29. Savichtcheva O, Debroas D, Kurmayer R, Villar C, Jenny JP, Arnaud F, Perga ME, Domaizon I. 2011. Quantitative PCR Enumeration of Total/Toxic Planktothrix rubescens and Total Cyanobacteria in Preserved DNA Isolated from Lake Sediments. Applied and Environmental Microbiology 77:8744-8753.
30. Pander B, Harris G, Scott DJ, Winzer K, Kopke M, Simpson SD, Minton NP, Henstra AM. 2019. The carbonic anhydrase of Clostridium autoethanogenum represents a new subclass of beta-carbonic anhydrases. Applied Microbiology and Biotechnology 103:7275-7286.
31. Salah Ud-Din AIM, Roujeinikova A. 2017. Methyl-accepting chemotaxis proteins: a core sensing element in prokaryotes and archaea. Cellular and Molecular Life Sciences 74:3293-3303.
32. Smith KS, Ferry JG. 2000. Prokaryotic carbonic anhydrases. Fems Microbiology Reviews 24:335-366.
33. Kozliak EI, Guilloton MB, Geraminejad M, Fuchs JA, Anderson PM. 1994. EXPRESSION OF PROTEINS ENCODED BY THE ESCHERICHIA-COLI CYN OPERON - CARBON DIOXIDE-ENHANCED DEGRADATION OF CARBONIC-ANHYDRASE. Journal of Bacteriology 176:5711-5717.
34. Charubin K, Modla S, Caplan JL, Papoutsakis ET. 2020. Interspecies Microbial Fusion and Large-Scale Exchange of Cytoplasmic Proteins and RNA in a Syntrophic Clostridium Coculture. Mbio 11:e02030-20.

35. Charubin K, Streett H, Papoutsakis ET. 2020. Development of Strong Anaerobic Fluorescent Reporters for Clostridium acetobutylicum and Clostridium ljungdahlii Using HaloTag and SNAP-tag Proteins. Applied and Environmental Microbiology 86:e01271-20.
36. Beliveau BJ, Joyce EF, Apostolopoulos N, Yilmaz F, Fonseka CY, McCole RB, Chang Y, Li JB, Senaratne TN, Williams BR, Rouillard JM, Wu CT. 2012. Versatile design and synthesis platform for visualizing genomes with Oligopaint FISH probes. Proceedings of the National Academy of Sciences 109:21301-21306.
37. Beliveau BJ, Apostolopoulos N, Wu CT. 2014. Visualizing Genomes with Oligopaint FISH Probes. Current Protocols in Molecular Biology 105.
38. Beliveau BJ, Kishi JY, Nir G, Sasaki HM, Saka SK, Nguyen SC, Wu C-T, Yin P. 2018. OligoMiner provides a rapid, flexible environment for the design of genome-scale oligonucleotide in situ hybridization probes. Proceedings of the National Academy of Sciences 115:E2183-E2192.
39. Beliveau BJ, Boettiger AN, Nir G, Bintu B, Yin P, Zhuang X, Wu CT. 2017. In Situ Super-Resolution Imaging of Genomic DNA with OligoSTORM and OligoDNA-PAINT, p 231-252 doi:10.1007/978-1-4939-7265-4_19. Springer New York.
40. Van Opijnen T, Bodi KL, Camilli A. 2009. Tn-seq: high-throughput parallel sequencing for fitness and genetic interaction studies in microorganisms. Nature Methods 6:767-772.
41. Woods C, Humphreys CM, Tomi-Andrino C, Henstra AM, Köpke M, Simpson SD, Winzer K, Minton NP. 2021. Application of transposon-insertion sequencing to determine gene essentiality in the acetogen Clostridium autoethanogenum doi:10.1101/2021.05.19.444907. Cold Spring Harbor Laboratory.
42. Goodman AL, McNulty NP, Zhao Y, Leip D, Mitra RD, Lozupone CA, Knight R, Gordon JI. 2009. Identifying genetic determinants needed to establish a human gut symbiont in its habitat. Cell Host Microbe 6:279-89.
43. Woods C, Humphreys CM, Tomi-Andrino C, Henstra AM, Köpke M, Simpson SD, Winzer K, Minton NP. 2022. Required gene set for autotrophic growth of Clostridium autoethanogenum. Applied and Environmental Microbiology:e02479-21.